Entropy stability for the compressible Navier-Stokes equations with strong imposition of the no-slip boundary condition

Anita Gjesteland *, Magnus Svärd

Department of Mathematics, University of Bergen, Postbox 7800, 5020 Bergen, Norway

ABSTRACT

We consider the compressible Navier-Stokes equations subject to no-slip adiabatic wall boundary conditions. The main goal is to investigate stability properties of schemes imposing the no-slip condition strongly (injection) and the temperature condition weakly by a simultaneous approximation term. To this end, we propose a low-order summation-by-parts scheme. By verifying the complete linearisation procedure, we prove linear stability for the scheme. In addition, and assuming that the interior scheme is entropy stable, we also prove entropy stability for the full scheme including the boundary treatment. Furthermore, we propose a linearly stable 3rd-order scheme with the same imposition of the wall conditions. However, the 3rd-order scheme is not provably non-linearly stable. A number of simulations show that the boundary procedure is robust for both schemes.

1. Introduction

The compressible Navier-Stokes equations describe the motion of a compressible, viscous and heat conducting fluid. Together with appropriate boundary and initial conditions, they model e.g. aerodynamic problems. Here, we consider the case where the fluid is interacting with solid walls. At walls, the equations are augmented with the no-slip condition leading to the formation of boundary layers that may become unstable and even generate turbulence. These complex phenomena are often studied using computational fluid dynamics. To reliably obtain accurate numerical approximations, the problem must be well-posed and its discrete approximation scheme stable. Unfortunately, well-posedness is, by and large, unknown for the Navier-Stokes equations. However, for smooth solutions, [24] ensures that numerical solutions produced by linearly stable schemes converge.

Linear theory is well developed and one can readily employ the energy method to prove well-posedness of initial-boundary-value problems (IBVP) (see e.g. [8]). Since the continuous energy method relies heavily on the integration-by-parts rule, spatial operators that satisfy the corresponding discrete property, summation-by-parts (SBP), have been developed (see e.g. [14], [29], [5]). These are used to prove energy stability and convergence of linear schemes ([9]). The linear theory has successfully been used to design schemes appropriate for subsonic smooth flows.

In the non-linear regime, however, the linear theory is not sufficient to guarantee stability, let alone well-posedness. To obtain non-linear bounds on the solution, the second law of thermodynamics, stating that the entropy within a closed system cannot decrease, can be used. In mathematical terms, this takes the form of an additional inequality and solutions that satisfy this inequality are termed entropy solutions (see Harten [10] and Tadmor [32] for the Cauchy problem and

---

* Corresponding author.
  E-mail addresses: anita.gjesteland@uib.no (A. Gjesteland), magnus.svard@uib.no (M. Svärd).

[23,27] for boundary treatments). Analogously, a numerical scheme is termed *entropy stable* if it satisfies a discrete equivalent of the continuous entropy inequality.

For both linear and non-linear problems, special attention must be paid to the boundaries, to ensure stability of the numerical scheme. SBP operators, together with the simultaneous approximation terms (SAT) to weakly impose boundary conditions, are applicable to a large class of problems, and are frequently used in the literature see [2,30,29,5,4,23,31]). In contrast to SAT, the injection method, which is the topic of this article, imposes the boundary conditions strongly. In practice, it does so by overwriting the boundary nodes with the boundary data after each time step (and/or Runge-Kutta stage). The injection method is appealing due to its simple nature, but may lead to unstable schemes (see e.g. [8,21]).

Here, we study SBP finite difference discretisations of the compressible Navier-Stokes equations augmented with the no-slip, i.e., homogeneous Dirichlet, boundary condition for the velocities and a homogeneous Neumann condition for the temperature. The no-slip condition is implemented strongly using the injection method, while the Neumann condition is implemented weakly with the SAT technique. Our primary objective is to demonstrate that this boundary procedure is entropy stable. Furthermore, this combination of boundary procedures has previously been considered in [22], where a stability proof for the symmetrised, constant-coefficient Navier-Stokes equations in two spatial dimensions was given. Our secondary objective is to investigate the nature of such linear stability proofs. Hence, we study the complete chain of arguments, from the linearisation of the full non-linear approximation scheme to a variable-coefficient problem and on to a symmetrisable frozen-coefficient problem. In particular, we focus on the validity of the last step.

The remaining article is organised as follows. First, we introduce linear well-posedness and stability, before we introduce the SBP operators and provide an example of the injection technique. Next, we review the linear well-posedness theory for the Navier-Stokes system. Thereafter, we prove stability for a scheme approximating the symmetric constant-coefficient version of the Navier-Stokes equations. (This is what is commonly referred to as linear stability analysis.) Next, we introduce the numerical scheme approximating the non-linear equations, and analyse its linear stability. In particular, we relate it to the constant-coefficient scheme. Next, we prove entropy stability of the scheme in one and two spatial dimensions. Lastly, we provide some numerical simulations that substantiate the findings of our stability proofs.

2. Preliminaries for the linear analysis

A general variable-coefficient initial-boundary-value problem (IBVP) can be written as

$$
\begin{aligned}
\frac{\partial u}{\partial t} &= P(\partial_x, x, t)u + F(x, t), \quad 0 < x < 1, \ t \geq 0, \\
Lu &= g(t), \\
u(x, 0) &= f(x),
\end{aligned}
\tag{1}
$$

where P is a spatial differential operator; F is a forcing function and L is an operator acting on the boundary. We will also need the standard L^2-norm defined by $\|u\|^2 = \int_0^1 |u|^2 \, dx$.

Definition 2.1 (*Well-posedness, [8]*). The initial-boundary-value problem (1) is **well-posed** if for $F = g = 0$ there exists a unique solution satisfying

$$\|u(\cdot, t)\| \leq K e^{\alpha t} \|f(\cdot)\|,$$

where K and α are constants independent of $f(x)$. ⌐

Next, define a computational grid with $N + 1$ equidistant grid points on the domain $0 \leq x \leq 1$: $x_i = ih$, $h > 0$. Let $\boldsymbol{u}$, $\boldsymbol{f}$, $\boldsymbol{F}$ and $\boldsymbol{g}$ be grid functions corresponding to the continuous functions u, f, F and g, respectively. That is, $[\boldsymbol{u}(t)]_i$ is the approximation of $u(x_i, t)$ etc. Let

$$
\begin{aligned}
\frac{d\boldsymbol{u}}{dt} &= \mathcal{D}_h \boldsymbol{u} + \boldsymbol{F}, \\
\mathcal{B}\boldsymbol{u} &= \boldsymbol{g}(t), \\
\boldsymbol{u}(0) &= \boldsymbol{f},
\end{aligned}
\tag{2}
$$

be a semi-discrete approximation of the IBVP (1). $\mathcal{D}_h$ is an approximation of the differential operator, P, and $\mathcal{B}$ an approximation of the boundary operator, L. For the semi-discrete schemes, we use the discrete analog to the L^2-norm defined by $\|\boldsymbol{u}\|_H^2 = \boldsymbol{u}^T H \boldsymbol{u}$, where H is a symmetric positive-definite matrix with elements of size $\mathcal{O}(h)$. Herein, we only consider diagonal H matrices.

Definition 2.2 (*Stability, [8]*). The problem (2) is **stable** if for $\boldsymbol{F} = \boldsymbol{g} = 0$, the solution satisfies

$$\|\boldsymbol{u}(t)\|_H \leq K e^{\alpha t} \|\boldsymbol{f}\|_H,$$

where K and α are constants independent of $\boldsymbol{f}$ and h. ⌟

Stability of the semi-discrete scheme implies stability of the fully discrete scheme if the spatial scheme is advanced in time with an appropriate Runge-Kutta method (see [15] for a proof).

Remark. For many problems, stability in the sense of Definition 2.2 for the variable-coefficient problem follows from stability of the "frozen-coefficient" problem. This was stated as a Conjecture in [9] (page 82).

3. Spatial discretisation

An SBP operator approximating the first derivative takes the form $D = H^{-1}Q$, where the matrices have the following properties:

i) H is a symmetric positive-definite matrix with elements of $\mathcal{O}(h)$,
ii) Q is an *almost* skew-symmetric matrix, satisfying the relation $Q + Q^T = B = \text{diag}(-1, 0, \ldots, 0, 1)$.

(For an introduction to SBP operators, see for example the review papers [5,29].)

For concreteness, we use the (2,1)-SBP operator that is second-order accurate in the interior and first-order accurate on the boundary. The operator takes the form

$$D = \frac{1}{2h}\begin{pmatrix} -2 & 2 & 0 & \ldots \\ -1 & 0 & 1 & \ldots \\ & & \ddots & \\ & -1 & 0 & 1 \\ & 0 & -2 & 2 \end{pmatrix}, \quad Q = \frac{1}{2}\begin{pmatrix} -1 & 1 & 0 & \ldots \\ -1 & 0 & 1 & \ldots \\ & & \ddots & \\ & -1 & 0 & 1 \\ & 0 & -1 & 1 \end{pmatrix}, \tag{3}$$

and $H = h \cdot \text{diag}(1/2, 1, \ldots, 1, 1/2)$ (this operator can be found in e.g. [16]).

Example 3.1. To introduce the injection technique we consider the system of equations

$$\begin{aligned} u_t + v_x &= 0, \\ v_t + u_x - 2v_x &= 0, \end{aligned} \tag{4}$$

with the boundary condition $v = 0$ at $x = 1$ (neglecting the left boundary for simplicity), and the semi-discretisation

$$\boldsymbol{u}_t + D\boldsymbol{v} = 0, \tag{5}$$

$$\boldsymbol{v}_t + D\boldsymbol{u} - 2D\boldsymbol{v} = 0, \tag{6}$$

where $\boldsymbol{u}$ and $\boldsymbol{v}$ are the numerical solution vectors.

In the injection method, $v(1, t) = 0$ is enforced by $v_N = 0$. A common approach to enforce injection is to remove the equation for v_N from the scheme by removing the boundary element of the solution vector and the last row and column of the spatial differential operator, D (see e.g. [8]). However, for coupled systems such as (4) this may inadvertently introduce extra boundary conditions. Here, we enforce injection indirectly by approximating $(v_N)_t = 0$. To achieve this, we introduce a new operator by setting all elements in the last row of D in (3) to zero, i.e.,

$$\tilde{D} = \frac{1}{2h}\begin{pmatrix} -2 & 2 & 0 & \ldots & 0 \\ -1 & 0 & 1 & \ldots & 0 \\ & & \ddots & & \\ & -1 & 0 & 1 \\ & 0 & 0 & 0 \end{pmatrix}.$$

We term $\tilde{D}$ a *Dirichlet-SBP* operator. The Dirichlet-SBP operator satisfies a new SBP-type property replacing ii):

$$\tilde{Q} + \tilde{Q}^T = \tilde{B} = \begin{pmatrix} -1 & 0 & 0 & \ldots & 0 & 0 \\ 0 & 0 & 0 & \ldots & 0 & 0 \\ 0 & 0 & 0 & \ldots & 0 & 0 \\ \vdots & & & \ddots & & \vdots \\ & & & & 0 & \frac{1}{2} \\ 0 & 0 & 0 & \ldots & \frac{1}{2} & 0 \end{pmatrix}.$$

We alter the scheme (5)-(6), to take the boundary condition $v(1, t) = 0$ into account, as follows,

$$\boldsymbol{u}_t + D\boldsymbol{v} = 0, \tag{7}$$

$$\boldsymbol{v}_t + \tilde{D}\boldsymbol{u} - 2\tilde{D}\boldsymbol{v} = 0. \tag{8}$$

Note that the last row of the $\boldsymbol{v}$-equation is, $(v_N)_t = 0$. Thus, since $v_N(0) = 0$, it follows that $v_N(t) \equiv 0$. To prove that (7)-(8) is a stable scheme, we use the energy method (see e.g. [5,29]). For (7) we have

$$\frac{d}{dt}\|\boldsymbol{u}\|_H^2 = -2\boldsymbol{u}^T Q \boldsymbol{v},$$

and for (8), we obtain

$$\frac{d}{dt}\|\boldsymbol{v}\|_H^2 = -\boldsymbol{v}^T H\tilde{D}\boldsymbol{u} - (\boldsymbol{v}^T H\tilde{D}\boldsymbol{u})^T + 2\boldsymbol{v}^T H\tilde{D}\boldsymbol{v} + 2(\boldsymbol{v}^T H\tilde{D}\boldsymbol{v})^T,$$
$$= -2\boldsymbol{v}^T \tilde{Q}\boldsymbol{u} + 2\boldsymbol{v}^T (\tilde{Q} + \tilde{Q}^T)\boldsymbol{v} = -2\boldsymbol{v}^T \tilde{Q}\boldsymbol{u} + 2\boldsymbol{v}^T \tilde{B}\boldsymbol{v}.$$

Adding the two estimates (and neglecting the left boundary terms emerging from (7)), we obtain

$$\frac{d}{dt}\left(\|\boldsymbol{u}\|_H^2 + \|\boldsymbol{v}\|_H^2\right) = -2\boldsymbol{u}^T Q\boldsymbol{v} - 2\boldsymbol{v}^T \tilde{Q}\boldsymbol{u} - 2v_0^2 + 2v_N v_{N-1}. \tag{9}$$

Since $v_N \equiv 0$ the following relations hold: $v_N v_{N-1} = 0$, $\boldsymbol{v}^T \tilde{Q}\boldsymbol{u} = \boldsymbol{v}^T Q\boldsymbol{u}$ and $\boldsymbol{v}^T Q\boldsymbol{u} = \boldsymbol{v}^T(B - Q^T)\boldsymbol{u} = \boldsymbol{v}^T B\boldsymbol{u} - \boldsymbol{v}^T Q^T\boldsymbol{u} = -\boldsymbol{v}^T Q^T\boldsymbol{u}$. Furthermore, $-\boldsymbol{v}^T Q^T\boldsymbol{u} = -(\boldsymbol{u}^T Q\boldsymbol{v})^T$, and we conclude that $\boldsymbol{v}^T \tilde{Q}\boldsymbol{u} = -\boldsymbol{u}^T Q\boldsymbol{v}$. Hence, the two first terms on the right-hand side of (9) cancel, and our estimate reads

$$\frac{d}{dt}\left(\|\boldsymbol{u}\|_H^2 + \|\boldsymbol{v}\|_H^2\right) = -2v_0^2 \leq 0,$$

which demonstrates that the semi-discrete scheme (7)-(8) is stable.

Remark. Note that the Dirichlet-SBP operator, $\tilde{D}$, need not be implemented. The same result is achieved by using D everywhere in (7)-(8) and setting $v_N = 0$ after each Runge-Kutta stage. ⌟

4. The linearised compressible Navier-Stokes equations

Consider the compressible Navier-Stokes equations in one spatial dimension. These can be stated as

$$\mathsf{u}_t + \mathsf{f}^{\mathsf{I}}(\mathsf{u})_x = \mathsf{f}^{\mathsf{v}}(\mathsf{u}, \mathsf{u}_x)_x, \qquad x \in \Omega = (0, 1), \quad 0 < t < \mathcal{T}, \tag{10}$$

where $\mathsf{u} = (\rho, m, E)^T$ are the conserved variables density, momentum ($m = \rho v$) and energy, and v denotes the velocity. $\mathsf{f}^{\mathsf{I}} = \left(m, \rho v^2 + p, v(E + p)\right)^T$, is the inviscid flux where p denotes the pressure, which is related to the conserved quantities through $p = (\gamma - 1)\left(E - \frac{1}{2}\rho v^2\right)$, where $\gamma = \frac{c_p}{c_v}$ is the ratio of the specific heats at constant pressure and volume. Furthermore, $\mathsf{f}^{\mathsf{v}} = (0, (2\mu + \lambda)v_x, (2\mu + \lambda)vv_x + \kappa \mathsf{T}_x)^T$ is the viscous flux, where T denotes the temperature, given by the ideal gas law $\mathsf{T} = \frac{p}{\mathcal{R}\rho}$, where $\mathcal{R}$ is the gas constant. Moreover, μ and λ denote the viscosity parameters, and we assume Stokes hypothesis, $\lambda = -\frac{2}{3}\mu$, with $\mu > 0$. Lastly, κ denotes the thermal conductivity. (Below, we use c to denote the speed of sound.) The equations are augmented with the adiabatic wall boundary conditions,

$$v = 0 \text{ (no-slip) and, } \quad \mathsf{T}_x = 0. \tag{11}$$

To investigate linear well-posedness, the system (10) may be linearised and subsequently symmetrised with the symmetrising matrices found in [1]. (Since the details of the derivations are omitted in [1], we include them in Appendix A.1 for the reader's convenience.)

We repeat this procedure briefly. To linearise the equations, we decompose the primitive variables, $\mathsf{v} = (\rho, v, p)^T$, into their exact (known smooth and bounded) solution and a small smooth perturbation, e.g. $\rho = \rho_{\text{ex}} + \rho'$, which yields a variable-coefficient problem. Then, we freeze the coefficients. Well-posedness of the variable-coefficient problem follows if all admissible frozen-coefficient problems are well-posed (see [9,13] for further information). The resulting linearised constant-coefficient problem is

$$\rho_t' + v^*\rho_x' + \rho^* v_x' = 0,$$
$$v_t' + v^* v_x' + \frac{1}{\rho^*}p_x' = \frac{2\mu + \lambda}{\rho^*}v_{xx}',$$
$$p_t' + \gamma p^* v_x' + v^* p_x' = -\frac{\gamma\mu p^*}{\mathrm{Pr}\rho^{*2}}\rho_{xx}' + \frac{\gamma\mu}{\mathrm{Pr}\rho^*}p_{xx}', \tag{12}$$

where the star superscript, '$*$', indicates a frozen coefficient. Finally, we symmetrise the equations using the matrices S_p and S_p^{-1} from [1]. Using the linearised gas law (see Appendix A.2), we obtain

$$\mathsf{w}_t + \mathcal{A}\mathsf{w}_x = \mathcal{B}\mathsf{w}_{xx}, \tag{13}$$

where

$$\mathsf{w} = \left(\frac{c^*}{\sqrt{\gamma}\rho^*}\rho', \ v', \ \frac{\gamma\mathcal{R}}{c^*\sqrt{\gamma}\sqrt{\gamma-1}}\mathrm{T}' \right)^T$$

and

$$\mathcal{A} = \begin{pmatrix} v^* & \frac{c^*}{\sqrt{\gamma}} & 0 \\ \frac{c^*}{\sqrt{\gamma}} & v^* & \sqrt{\frac{\gamma-1}{\gamma}}c^* \\ 0 & \sqrt{\frac{\gamma-1}{\gamma}}c^* & v^* \end{pmatrix}, \quad \mathcal{B} = \begin{pmatrix} 0 & 0 & 0 \\ 0 & \frac{2\mu+\lambda}{\rho^*} & 0 \\ 0 & 0 & \frac{\gamma\mu}{\mathrm{Pr}\rho^*} \end{pmatrix},$$

with $\mathrm{Pr} = \frac{c_p\mu}{\kappa}$ denoting the Prandtl number and $c_p = \frac{\gamma\mathcal{R}}{\gamma-1}$.

For completeness, we proceed by reviewing the well-posedness analysis found in e.g. [28]. Consider (13) on the spatial domain $\Omega = (0, 1)$ with L^2-bounded initial data. The linearised boundary conditions (11), take the form

$$v'(\{0, 1\}, t) = 0, \quad v^*(\{0, 1\}, t) = 0, \quad \mathrm{T}'_x(\{0, 1\}, t) = 0. \tag{14}$$

(Note that admissible solutions satisfy the no-slip condition, whence $v^*(\{0, 1\}, t) = 0$.) The energy method and (14) lead to

$$\frac{d}{dt}\|\mathsf{w}\|^2 + 2\int_\Omega \mathsf{w}_x^T \mathcal{B}\mathsf{w}_x \, dx = 2\mathsf{w}^T \mathcal{B}\mathsf{w}_x|_0^1 - \mathsf{w}^T \mathcal{A}\mathsf{w}|_0^1 = 0.$$

Hence our problem is well-posed in the sense of Definition 2.1.

Remark. The Dirichlet condition $\mathrm{T}'(\{0, 1\}) = 0$ would give the same result, but since the non-linear analysis later in this article requires $\mathrm{T}'_x(\{0, 1\}) = 0$, we only consider the latter.

4.1. The semi-discrete scheme

Turning to the semi-discretisation of the problem (12) subject to the boundary conditions (14), we divide the spatial domain into $N + 1$ equidistant grid points with grid spacing $h = 1/N$. Bold-face letters denote the numerical solution vectors.

To enforce the no-slip condition at both boundaries, the Dirichlet-SBP operator is defined by

$$\tilde{D} = \frac{1}{2h}\begin{pmatrix} 0 & 0 & 0 & \dots & & \\ -1 & 0 & 1 & \dots & & \\ & & \ddots & & & \\ & & -1 & 0 & 1 & \\ & & & 0 & 0 & 0 \end{pmatrix}, \quad \tilde{B} = \tilde{Q} + \tilde{Q}^T = \begin{pmatrix} 0 & -\frac{1}{2} & 0 & \dots & 0 & 0 \\ -\frac{1}{2} & 0 & 0 & \dots & 0 & 0 \\ 0 & 0 & 0 & \dots & 0 & 0 \\ \vdots & & & \ddots & & \vdots \\ & & & & 0 & \frac{1}{2} \\ 0 & 0 & 0 & \dots & \frac{1}{2} & 0 \end{pmatrix}. \tag{15}$$

We introduce $\hat{\boldsymbol{\rho}} = \frac{c^*}{\sqrt{\gamma}\rho^*}\rho'$ and $\hat{\mathrm{T}} = -\frac{c^*}{\rho^*\sqrt{\gamma}\sqrt{\gamma-1}}\rho' + \sqrt{\frac{\gamma}{\gamma-1}}\frac{1}{\rho^*c^*}\boldsymbol{p}' = \frac{\gamma\mathcal{R}}{c^*\sqrt{\gamma}\sqrt{\gamma-1}}\mathrm{T}'$ and consider the following semi-discrete numerical scheme to approximate the system (12).

$$\hat{\boldsymbol{\rho}}_t + v^* D\hat{\boldsymbol{\rho}} + \frac{c^*}{\sqrt{\gamma}}D\boldsymbol{v}' = 0, \tag{16}$$

$$\boldsymbol{v}'_t + \frac{c^*}{\sqrt{\gamma}}\tilde{D}\hat{\boldsymbol{\rho}} + v^*\tilde{D}\boldsymbol{v}' + \sqrt{\frac{\gamma-1}{\gamma}}c^*\tilde{D}\hat{\mathrm{T}} = \frac{2\mu+\lambda}{\rho^*}\tilde{D}D\boldsymbol{v}', \tag{17}$$

$$\hat{\mathrm{T}}_t + \sqrt{\frac{\gamma-1}{\gamma}}c^* D\boldsymbol{v}' + v^* D\hat{\mathrm{T}} = \frac{\gamma\mu}{\mathrm{Pr}\rho^*}DD\hat{\mathrm{T}} + \mathsf{SAT}, \tag{18}$$

where

$$\mathsf{SAT} = -\frac{\gamma\mu}{\mathrm{Pr}\rho^*}H^{-1}B(D\hat{\mathrm{T}} - 0), \tag{19}$$

imposes the homogeneous Neumann condition for the temperature weakly. We observe the following

- Since $v' \equiv 0$ at the boundaries initially, the use of the Dirichlet-SBP operator, $\tilde{D}$, in (17) ensures that v'_0, v'_N remains zero for all $t \geq 0$.
- Note that in (16) and (18), $\hat{\rho}_{0,N}$ and $\hat{\mathbb{T}}_{0,N}$ are unknowns that are updated in time.
- Note that the Dirichlet-SBP operator is applied only once for the second-derivative approximation in the right-hand side of (17). Using the Dirichlet-SBP operator twice would inadvertently impose the improper boundary condition $v'_x = 0$.
- When implementing the scheme, the $\tilde{D}$ is not necessary. One can equivalently compute all derivatives using D and reset the velocity to zero after each Runge-Kutta stage.

Remark. A similar scheme for the non-dimensional linearised and symmetrised Navier-Stokes equations was demonstrated to be stable using SAT to impose the no-slip conditions in [28]. The modifications of the SBP operator described here only affect the wall boundaries. Far-field boundaries may be handled in a stable manner using SAT, see [30].

Proposition 4.1. *The semi-discrete scheme* (16) - (18) *is energy stable.*

Remark. Linear stability of a numerical scheme using the injection method for imposing the no-slip condition and SAT to impose the temperature condition for the linearised and symmetrised constant-coefficient problem (13) was proven in [22]. However, in the present analysis, we use a different methodology for the injection method.

Proof. We carry out the energy analysis for each equation separately, before adding the three preliminary results to obtain the final energy estimate. (We neglect the right boundary for the rest of this analysis to reduce notation. Its treatment resembles the left boundary.) For (16), we obtain

$$\frac{d}{dt}\|\hat{\boldsymbol{\rho}}\|_H^2 = -v^* \hat{\boldsymbol{\rho}}^T (Q + Q^T)\hat{\boldsymbol{\rho}} - 2\frac{c^*}{\sqrt{\gamma}}\hat{\boldsymbol{\rho}}^T Q \boldsymbol{v}'.$$

Utilising the SBP-properties and subsequently $v^* = 0$ yield

$$\frac{d}{dt}\|\hat{\boldsymbol{\rho}}\|_H^2 = v^* \hat{\rho}_0^2 - 2\frac{c^*}{\sqrt{\gamma}}\hat{\boldsymbol{\rho}}^T Q \boldsymbol{v}' = -2\frac{c^*}{\sqrt{\gamma}}\hat{\boldsymbol{\rho}}^T Q \boldsymbol{v}'. \tag{20}$$

Next, Equation (17) results in

$$\frac{d}{dt}\|\boldsymbol{v}'\|_H^2 = -2\frac{c^*}{\sqrt{\gamma}}\boldsymbol{v}'^T \tilde{Q}\hat{\boldsymbol{\rho}} - 2\sqrt{\frac{\gamma-1}{\gamma}}c^*\boldsymbol{v}'^T \tilde{Q}\hat{\mathbb{T}} \underbrace{-v^*\boldsymbol{v}'^T(\tilde{Q} + \tilde{Q}^T)\boldsymbol{v}' + 2\frac{2\mu+\lambda}{\rho^*}\boldsymbol{v}'^T \tilde{Q} D\boldsymbol{v}'}_{A_1}. \tag{21}$$

Using (15), we obtain

$$A_1 = -v^*\boldsymbol{v}'^T \tilde{B}\boldsymbol{v}' + 2\frac{2\mu+\lambda}{\rho^*}\boldsymbol{v}'^T(\tilde{B} - \tilde{Q}^T)D\boldsymbol{v}', = v^* v'_0 v'_1 + \frac{2\mu+\lambda}{\rho^*}\left(-v'_1(D\boldsymbol{v}')_0 - v'_0(D\boldsymbol{v}')_1 - 2(\tilde{D}\boldsymbol{v}')^T HD\boldsymbol{v}'\right),$$

and, using $v'_0 = 0$,

$$A_1 = \frac{2\mu+\lambda}{\rho^*}\left(-v'_1\frac{v'_1 - v'_0}{h} - 2(\tilde{D}\boldsymbol{v}')^T HD\boldsymbol{v}'\right) \leq -\frac{2\mu+\lambda}{\rho^*}\left(2(\tilde{D}\boldsymbol{v}')^T HD\boldsymbol{v}'\right).$$

The estimate (21) therefore reduces to

$$\frac{d}{dt}\|\boldsymbol{v}'\|_H^2 \leq -2\frac{c^*}{\sqrt{\gamma}}\boldsymbol{v}'^T \tilde{Q}\hat{\boldsymbol{\rho}} - 2\sqrt{\frac{\gamma-1}{\gamma}}c^*\boldsymbol{v}'^T \tilde{Q}\hat{\mathbb{T}} - 2\frac{2\mu+\lambda}{\rho^*}(\tilde{D}\boldsymbol{v}')^T HD\boldsymbol{v}'. \tag{22}$$

The energy method for (18) with (19) gives

$$\frac{d}{dt}\|\hat{\mathbb{T}}\|_H^2 = -2\sqrt{\frac{\gamma-1}{\gamma}}c^*\hat{\mathbb{T}}Q\boldsymbol{v}' \underbrace{-v^*\hat{\mathbb{T}}^T(Q + Q^T)\hat{\mathbb{T}} + 2\frac{\gamma\mu}{\Pr\rho^*}\hat{\mathbb{T}}^T Q D\hat{\mathbb{T}} - 2\frac{\gamma\mu}{\Pr\rho^*}\hat{\mathbb{T}}^T BD\hat{\mathbb{T}}}_{A_2}. \tag{23}$$

Using $Q + Q^T = B$ and $v^* = 0$, yield

$$A_2 = v^*\hat{\mathbb{T}}_0^2 + 2\frac{\gamma\mu}{\Pr\rho^*}\left(\hat{\mathbb{T}}^T(B - Q^T)D\hat{\mathbb{T}} - \hat{\mathbb{T}}^T BD\hat{\mathbb{T}}\right) = v^*\hat{\mathbb{T}}_0^2 - 2\frac{\gamma\mu}{\Pr\rho^*}\hat{\mathbb{T}}^T Q^T D\hat{\mathbb{T}} = -2\frac{\gamma\mu}{\Pr\rho^*}(D\hat{\mathbb{T}})^T H(D\hat{\mathbb{T}}).$$

Hence, (23) results in

$$\frac{d}{dt}\|\hat{\mathbb{T}}\|_H^2 = -2\sqrt{\frac{\gamma-1}{\gamma}}c^*\hat{\mathbb{T}}^T Q \boldsymbol{v}' - 2\frac{\gamma\mu}{\Pr\rho^*}(D\hat{\mathbb{T}})^T H(D\hat{\mathbb{T}}). \tag{24}$$

We add all the preliminary estimates (20), (22) and (24) to obtain

$$
\frac{d}{dt}\left(\|\hat{\boldsymbol{\rho}}\|_H^2 + \|\boldsymbol{v}'\|_H^2 + \|\hat{\mathbb{T}}\|_H^2\right) \leq -2\frac{c^*}{\gamma}\left(\hat{\boldsymbol{\rho}}^T Q\,\boldsymbol{v}' + \boldsymbol{v}'^T\tilde{Q}\,\hat{\boldsymbol{\rho}}\right) - 2\sqrt{\frac{\gamma-1}{\gamma}}c^*\left(\boldsymbol{v}'^T\tilde{Q}\,\hat{\mathbb{T}} + \hat{\mathbb{T}}^T Q\,\boldsymbol{v}'\right)
$$
$$
-2\frac{2\mu+\lambda}{\rho}(\tilde{D}\boldsymbol{v}')^T H\tilde{D}\boldsymbol{v}' - 2\frac{\gamma\mu}{\mathrm{Pr}\rho}(D\hat{\mathbb{T}})^T H D\hat{\mathbb{T}}.
\tag{25}
$$

Consider the term $\boldsymbol{v}'^T\tilde{Q}\,\hat{\boldsymbol{\rho}}$. As in Example 3.1, it follows from $v_0' = v_N' \equiv 0$ that $\boldsymbol{v}'^T\tilde{Q}\,\hat{\boldsymbol{\rho}} \equiv \boldsymbol{v}'^T Q\,\hat{\boldsymbol{\rho}} = \boldsymbol{v}'^T B\hat{\boldsymbol{\rho}} - \boldsymbol{v}'^T Q^T\hat{\boldsymbol{\rho}} = -(\hat{\boldsymbol{\rho}}^T Q\,\boldsymbol{v}')^T$. Since $-(\hat{\boldsymbol{\rho}}^T Q\,\boldsymbol{v}')^T$ is a scalar we obtain $\boldsymbol{v}'^T\tilde{Q}\,\hat{\boldsymbol{\rho}} = -\hat{\boldsymbol{\rho}}^T Q\,\boldsymbol{v}'$. The same argument holds for the term $\boldsymbol{v}'^T\tilde{Q}\,\hat{\mathbb{T}}$, and the two first terms in (25) therefore vanish. Lastly, since $(\tilde{D}\boldsymbol{v}')_0 = 0$, we have $(\tilde{D}\boldsymbol{v}')^T H D\boldsymbol{v}' = (\tilde{D}\boldsymbol{v}')^T H\tilde{D}\boldsymbol{v}'$, and we obtain

$$
\frac{d}{dt}\left(\|\hat{\boldsymbol{\rho}}\|_H^2 + \|\boldsymbol{v}'\|_H^2 + \|\hat{\mathbb{T}}\|_H^2\right) + 2\frac{2\mu+\lambda}{\rho^*}\|\tilde{D}\boldsymbol{v}\|_H^2 + 2\frac{\gamma\mu}{\mathrm{Pr}\rho^*}\|D\hat{\mathbb{T}}\|_H^2 \leq 0.
\tag{26}
$$

Hence, the scheme is stable in the sense of Definition 2.2. $\square$

5. The non-linear Navier-Stokes equations

The semi-discrete scheme approximating (10) is given by

$$
\mathbf{u}_t + \mathcal{D}^{\mathsf{I}}\mathbf{f}^{\mathsf{I}} = \mathcal{D}^{\mathsf{V}}\mathbf{f}^{\mathsf{V}} + \mathsf{SAT},
\tag{27}
$$

where $\mathbf{u} = (\boldsymbol{\rho}, \boldsymbol{v}, \boldsymbol{E})^T$ is the numerical solution vector. The convective term of (10) is, once again ignoring the right boundary, approximated by

$$
(\mathcal{D}^{\mathsf{I}}\mathbf{f}^{\mathsf{I}})_i = \begin{cases} \frac{\mathbf{f}_{1/2}^{\mathsf{I}} - \mathbf{f}_0^{\mathsf{I}}}{h/2}, & i = 0, \\ \frac{\mathbf{f}_{i+1/2}^{\mathsf{I}} - \mathbf{f}_{i-1/2}^{\mathsf{I}}}{h}, & i = 1, \ldots, N-1, \end{cases}
\tag{28}
$$

where

$$
\mathbf{f}_{i+1/2}^{\mathsf{I}} = \frac{\mathbf{f}_{i+1}^{\mathsf{I}} + \mathbf{f}_i^{\mathsf{I}}}{2} - \frac{\delta_{i+1/2}\,(\mathbf{u}_{i+1} - \mathbf{u}_i)}{2}
\tag{29}
$$

is the approximation of the inviscid flux and $\mathbf{f}_i^{\mathsf{I}} = \mathbf{f}^{\mathsf{I}}(\mathbf{u}_i)$. The second term is artificial diffusion and for δ sufficiently large, the approximation is entropy stable in the sense of (52) below (see also [32]). Furthermore, the components of $\mathbf{f}_0^{\mathsf{I}}$ are

$$
\mathbf{f}_0^{\mathsf{I},\rho} = (\boldsymbol{\rho}.\boldsymbol{v})_0,
\tag{30}
$$
$$
\mathbf{f}_0^{\mathsf{I},m} = \mathbf{f}_{1/2}^{\mathsf{I},m},
\tag{31}
$$
$$
\mathbf{f}_0^{\mathsf{I},E} = (\boldsymbol{v}.(\boldsymbol{E} + \boldsymbol{p}))_0,
\tag{32}
$$

where the superscripts ρ, m, E denote which equation the vector element corresponds to, and the dot symbolises element-wise vector multiplications.

Remark. Note that (31) implies that the flux difference (28) is identically equal to zero at grid point x_0 for the momentum equation.

Next, the diffusive term of (10) is conveniently approximated on matrix form by

$$
\mathcal{D}^{\mathsf{V}}\mathbf{f}^{\mathsf{V}} = \left(0, \tilde{D}((2\mu+\lambda)D\boldsymbol{v}), D((2\mu+\lambda)\overset{b,x}{\boldsymbol{v}}.D\boldsymbol{v} + \kappa D\mathbb{T})\right)^T,
\tag{33}
$$

(the definition of $\overset{b,x}{\boldsymbol{v}}.D\boldsymbol{v}$ is given in (36)-(37)) and the SAT is given by

$$
\mathsf{SAT} = \left(0, 0, -\kappa H^{-1}B(D\mathbb{T} - 0)\right)^T.
\tag{34}
$$

Remark. The scheme for the momentum equation is $m_t = 0$ on the boundary, i.e., $m_0(t) \equiv 0$ such that $v_0 \equiv 0$ for all $t \geq 0$.

Remark. It is also possible to handle a heat-entropy flow boundary condition, where the temperature condition in (11) is replaced with $\kappa\frac{\mathbb{T}_x}{\mathbb{T}} = g$. The corresponding SAT would then take the form $\mathsf{SAT} = H^{-1}(\kappa BD\mathbb{T} - \mathbb{T}g)$, which would yield an entropy stable scheme for appropriately chosen g.

In (33) we use

$$(D(\boldsymbol{a}.\boldsymbol{b}))_i = \begin{cases} \frac{a_1 b_1 - a_0 b_0}{h} = a_1 (D\boldsymbol{b})_0 + b_0 (D\boldsymbol{a})_0 = b_1 (D\boldsymbol{a})_0 + a_0 (D\boldsymbol{b})_0 & i = 0, \\ \frac{a_{i+1} b_{i+1} - a_{i-1} b_{i-1}}{2h} = \frac{a_{i+1} + a_{i-1}}{2} (D\boldsymbol{b})_i + \frac{b_{i+1} + b_{i-1}}{2} (D\boldsymbol{a})_i & i = 1, \ldots, N-1, \\ \frac{a_N b_N - a_{N-1} b_{N-1}}{h} = a_N (D\boldsymbol{b})_N + b_{N-1} (D\boldsymbol{a})_N = b_N (D\boldsymbol{a})_N + a_N (D\boldsymbol{b})_N & i = N. \end{cases} \tag{35}$$

To distinguish between the two boundary rules, we introduce the following notation

$$\overset{b,x}{\boldsymbol{a}} = \begin{pmatrix} a_0, & \frac{a_2 + a_0}{2}, & \ldots, & \frac{a_N + a_{N-2}}{2}, & a_N \end{pmatrix}, \\ \overset{i,x}{\boldsymbol{a}} = \begin{pmatrix} a_1, & \frac{a_2 + a_0}{2}, & \ldots, & \frac{a_N + a_{N-2}}{2}, & a_{N-1} \end{pmatrix}, \tag{36}$$

and

$$\left(\overset{b,x}{\boldsymbol{a}}.(D\boldsymbol{b}) \right)_i = \begin{cases} a_0 (D\boldsymbol{b})_0, & i = 0, \\ \frac{a_{i+1} + a_{i-1}}{2} (D\boldsymbol{b})_i, & i = 1, \ldots N-1, \\ a_N (D\boldsymbol{b})_N, & i = N, \end{cases} \tag{37}$$

$$\left(\overset{i,x}{\boldsymbol{a}}.(D\boldsymbol{b}) \right)_i = \begin{cases} a_1 (D\boldsymbol{b})_0, & i = 0, \\ \frac{a_{i+1} + a_{i-1}}{2} (D\boldsymbol{b})_i, & i = 1, \ldots N-1, \\ a_{N-1} (D\boldsymbol{b})_N, & i = N. \end{cases} \tag{38}$$

Here, superscript b signifies that $\boldsymbol{a}$ is taken at the *boundary* node and superscript i signifies that $\boldsymbol{a}$ is taken at the first neighbouring *interior* node. A similar relation holds for the averages taken in the y-direction. Using (37) and (38), we can rewrite (35) as

$$D_x(\boldsymbol{a}.\boldsymbol{b}) = \overset{b,x}{\boldsymbol{a}}.(D_x\boldsymbol{b}) + \overset{i,x}{\boldsymbol{b}}.(D_x\boldsymbol{a}) = \overset{b,x}{\boldsymbol{b}}.(D_x\boldsymbol{a}) + \overset{i,x}{\boldsymbol{a}}.(D_x\boldsymbol{b}), \\ D_y(\boldsymbol{a}.\boldsymbol{b}) = \overset{b,y}{\boldsymbol{a}}.(D_y\boldsymbol{b}) + \overset{i,y}{\boldsymbol{b}}.(D_y\boldsymbol{a}) = \overset{b,y}{\boldsymbol{b}}.(D_y\boldsymbol{a}) + \overset{i,y}{\boldsymbol{a}}.(D_y\boldsymbol{b}), \tag{39}$$

where D_x and D_y approximate the x- and y-derivative, respectively.

Lastly, a similar rule holds for quotients

$$\left(D \left(\frac{\boldsymbol{a}}{\boldsymbol{b}} \right) \right)_i = \begin{cases} \frac{\frac{a_1}{b_1} - \frac{a_0}{b_0}}{h} = \frac{b_0 (D\boldsymbol{a})_0 - a_0 (D\boldsymbol{b})_0}{b_0 b_1} = \frac{b_1 (D\boldsymbol{a})_0 - a_1 (D\boldsymbol{b})_0}{b_0 b_1} & i = 0, \\ \frac{\frac{a_{i+1}}{b_{i+1}} - \frac{a_{i-1}}{b_{i-1}}}{2h} = \frac{1}{b_{i+1} b_{i-1}} \left(\frac{b_{i+1} + b_{i-1}}{2} (D\boldsymbol{a})_i - \frac{a_{i+1} + a_{i-1}}{2} (D\boldsymbol{b})_i \right), & i = 1, \ldots, N-1 \\ \frac{\frac{a_N}{b_N} - \frac{a_{N-1}}{b_{N-1}}}{h} = \frac{b_N (D\boldsymbol{a})_N - a_N (D\boldsymbol{b})_N}{b_N b_{N-1}} = \frac{b_{N-1} (D\boldsymbol{a})_N - a_{N-1} (D\boldsymbol{b})_N}{b_n b_{N-1}}, & i = N. \end{cases} \tag{40}$$

The inviscid term in (27) can equivalently be recast on matrix form. To this end, the artificial diffusion can be recognised as a second-derivative SBP operator with variable coefficients (see [18] and [19]). Define $D_2^{(\delta)} = H^{-1}(-D_{(\delta)}^T \tilde{\Delta} D_{(\delta)} + \bar{\Delta} S)$, where $D_2^{(\delta)}$, $D_{(\delta)}$, $\tilde{\Delta} = \frac{h}{2} \text{diag}(\delta_{1/2}, \delta_{3/2}, \ldots, \delta_{N-1/2})$ and $\bar{\Delta} = \text{diag}(-\delta_0, 0, \ldots, 0, \delta_N)$ correspond to the matrices D_2, D, $\tilde{B}$ and B, respectively, given in [18]. Then the artificial diffusion (AD) terms in (29) can be recast as

$$AD^\rho = -h H^{-1} D_{(\delta)}^T \tilde{\Delta} D_{(\delta)} \boldsymbol{\rho}, \\ AD^m = -h H^{-1} \tilde{D}_{(\delta)}^T \tilde{\Delta} D_{(\delta)} (\boldsymbol{\rho}.\boldsymbol{v}), \\ AD^E = -h H^{-1} D_{(\delta)}^T \tilde{\Delta} D_{(\delta)} \boldsymbol{E}, \tag{41}$$

where $\tilde{D}_{(\delta)}^T$ is the Dirichlet-SBP operator corresponding to $D_{(\delta)}^T$, i.e., it is $D_{(\delta)}^T$ with the elements of first and last row set to zero. Then, using the SBP operators (3) and (15), (28) can be restated as,

$$\mathcal{D}^{\mathsf{I}} \mathbf{f}^{\mathsf{I}} = \begin{pmatrix} D \mathbf{f}^{\mathsf{I},\rho} - AD^\rho \\ \tilde{D} \mathbf{f}^{\mathsf{I},m} - AD^m \\ D \mathbf{f}^{\mathsf{I},E} - AD^E \end{pmatrix}, \tag{42}$$

where $\mathbf{f}^{\mathsf{I},\rho} = \boldsymbol{\rho}.\boldsymbol{v}$, $\mathbf{f}^{\mathsf{I},m} = \boldsymbol{\rho}.\boldsymbol{v}.^2 + \boldsymbol{p}$, and $\mathbf{f}^{\mathsf{I},E} = \boldsymbol{v}.(\boldsymbol{E} + \boldsymbol{p})$.

5.1. Linear stability of the non-linear scheme

To demonstrate the linear stability of the scheme (27), we consider its linearisation and relate it to the scheme in Proposition (4.1). Using (41) and (42), the scheme (27) is recast as

$$\boldsymbol{\rho}_t + D(\boldsymbol{\rho}.\boldsymbol{v}) + hH^{-1}D_{(\delta)}^T\tilde{\Delta}D_{(\delta)}\boldsymbol{\rho} = 0,$$

$$(\boldsymbol{\rho}.\boldsymbol{v})_t + \tilde{D}(\boldsymbol{\rho}.\boldsymbol{v}.^2 + \boldsymbol{p}) + hH^{-1}\tilde{D}_{(\delta)}^T\tilde{\Delta}D_{(\delta)}(\boldsymbol{\rho}.\boldsymbol{v}) = (2\mu + \lambda)\tilde{D}D\boldsymbol{v}, \tag{43}$$

$$\boldsymbol{E}_t + D(\boldsymbol{v}.(\boldsymbol{E} + \boldsymbol{p})) + hH^{-1}D_{(\delta)}^T\tilde{\Delta}D_{(\delta)}\boldsymbol{E} = (2\mu + \lambda)D(\overset{b,x}{\boldsymbol{v}}.D\boldsymbol{v}) + \kappa(DD\mathrm{T} - H^{-1}BD\mathrm{T}).$$

In analogy with the continuous problem, we insert into the scheme the decomposition, $\boldsymbol{v}^T = (\boldsymbol{\rho}, \boldsymbol{v}, \boldsymbol{p}) = (\boldsymbol{\rho}_{\mathrm{ex}}, \boldsymbol{v}_{\mathrm{ex}}, \boldsymbol{p}_{\mathrm{ex}}) + (\boldsymbol{\rho}', \boldsymbol{v}', \boldsymbol{p}')$. (Smooth exact solution and a perturbation. Cf. Appendix A.1.) In the subsequent linearisation process, we neglect terms that are quadratically small in the perturbations and we omit zeroth-order terms since they do not affect stability (see [9]). The smooth exact solution satisfies the scheme up to a bounded truncation error, which is benign with respect to stability. Furthermore, linearisation of the variable-coefficient second-derivative approximations, yields terms on the form $D_{(\delta)}^T\tilde{\Delta}'D_{(\delta)}\boldsymbol{\beta}_{\mathrm{ex}}$ (where $\boldsymbol{\beta}_{\mathrm{ex}}$ is any of the independent variables). Due to the form of $\tilde{\Delta} \sim \boldsymbol{v} + \mathrm{T}$, these terms are bounded by the corresponding principal terms emanating from the momentum and energy equation. (All the terms that are assumed to be bounded or linear in the principal variable in the linearisation are denoted as $\mathcal{O}(1, \boldsymbol{v})$ in the derivations below.) The linearised equation scheme (43) becomes:

$$\boldsymbol{\rho}_t' + D(\boldsymbol{\rho}_{\mathrm{ex}}.\boldsymbol{v}' + \boldsymbol{\rho}'.\boldsymbol{v}_{\mathrm{ex}}) + hH^{-1}D_{(\delta)}^T\tilde{\Delta}D_{(\delta)}\boldsymbol{\rho}' = \mathcal{O}(1, \boldsymbol{v}),$$

$$\boldsymbol{v}_t' + \frac{1}{\boldsymbol{\rho}_{\mathrm{ex}}}.\tilde{D}(2\boldsymbol{\rho}_{\mathrm{ex}}.\boldsymbol{v}_{\mathrm{ex}}.\boldsymbol{v}' + \boldsymbol{\rho}'.\boldsymbol{v}_{\mathrm{ex}}.^2 + \boldsymbol{p}') - \frac{\boldsymbol{v}_{\mathrm{ex}}.}{\boldsymbol{\rho}_{\mathrm{ex}}}.D(\boldsymbol{\rho}_{\mathrm{ex}}.\boldsymbol{v}' + \boldsymbol{\rho}'.\boldsymbol{v}_{\mathrm{ex}})$$

$$-\frac{\boldsymbol{v}_{\mathrm{ex}}.}{\boldsymbol{\rho}_{\mathrm{ex}}}.hH^{-1}D_{(\delta)}^T\tilde{\Delta}D_{(\delta)}\boldsymbol{\rho}' + \frac{1}{\boldsymbol{\rho}_{\mathrm{ex}}}.hH^{-1}\tilde{D}_{(\delta)}^T\tilde{\Delta}D_{(\delta)}(\boldsymbol{\rho}_{\mathrm{ex}}.\boldsymbol{v}' + \boldsymbol{\rho}'.\boldsymbol{v}_{\mathrm{ex}}) = \frac{2\mu + \lambda}{\boldsymbol{\rho}_{\mathrm{ex}}}.\tilde{D}D\boldsymbol{v}' + \mathcal{O}(1, \boldsymbol{v}),$$

$$\frac{\boldsymbol{p}_t'}{\gamma - 1} + \frac{1}{2}\boldsymbol{v}_{\mathrm{ex}}.^2 D(\boldsymbol{\rho}_{\mathrm{ex}}.\boldsymbol{v}' + \boldsymbol{\rho}'.\boldsymbol{v}_{\mathrm{ex}}) - \boldsymbol{v}_{\mathrm{ex}}.\tilde{D}(2\boldsymbol{\rho}_{\mathrm{ex}}.\boldsymbol{v}_{\mathrm{ex}}.\boldsymbol{v}' + \boldsymbol{\rho}'\boldsymbol{v}_{\mathrm{ex}}.^2 + \boldsymbol{p}')$$

$$+ D\left(\frac{\gamma}{\gamma-1}(\boldsymbol{v}'\boldsymbol{p}_{\mathrm{ex}} + \boldsymbol{v}_{\mathrm{ex}}\boldsymbol{p}') + \frac{3}{2}\boldsymbol{\rho}_{\mathrm{ex}}.\boldsymbol{v}_{\mathrm{ex}}.\boldsymbol{v}' + \frac{1}{2}\boldsymbol{\rho}'\boldsymbol{v}_{\mathrm{ex}}.^3\right)$$

$$+ \frac{1}{2}\boldsymbol{v}_{\mathrm{ex}}.^2 hH^{-1}D_{(\delta)}^T\tilde{\Delta}D_{(\delta)}\boldsymbol{\rho}' - \boldsymbol{v}_{\mathrm{ex}}.hH^{-1}\tilde{D}_{(\delta)}^T\tilde{\Delta}D_{(\delta)}(\boldsymbol{\rho}_{\mathrm{ex}}.\boldsymbol{v}' + \boldsymbol{\rho}'.\boldsymbol{v}_{\mathrm{ex}})$$

$$+ hH^{-1}D_{(\delta)}^T\tilde{\Delta}D_{(\delta)}(\frac{\boldsymbol{p}'}{\gamma-1} + \boldsymbol{\rho}_{\mathrm{ex}}.\boldsymbol{v}_{\mathrm{ex}}.\boldsymbol{v}' + \frac{1}{2}\boldsymbol{\rho}'.\boldsymbol{v}_{\mathrm{ex}}.^2) = (2\mu + \lambda)\left(D(\overset{b,x}{\boldsymbol{v}}_{\mathrm{ex}}.D\boldsymbol{v}') - \boldsymbol{v}_{\mathrm{ex}}.\tilde{D}D\boldsymbol{v}'\right)$$

$$+ \frac{\kappa}{\mathcal{R}}\left(DD\left(\frac{\boldsymbol{p}'.}{\boldsymbol{\rho}_{\mathrm{ex}}} - \frac{\boldsymbol{p}_{\mathrm{ex}}.\boldsymbol{\rho}'.}{\boldsymbol{\rho}_{\mathrm{ex}}.^2}\right)\right.$$

$$\left.- H^{-1}BD\left(\frac{\boldsymbol{p}'.}{\boldsymbol{\rho}_{\mathrm{ex}}} - \frac{\boldsymbol{p}_{\mathrm{ex}}.\boldsymbol{\rho}'.}{\boldsymbol{\rho}_{\mathrm{ex}}.^2}\right)\right) + \mathcal{O}(1, \boldsymbol{v}).$$

Next, we use a result found in the proof of Lemma 2.2 of [20]: For a known continuously differentiable function, $a_{\mathrm{ex}}(x, t)$,

$$D(\boldsymbol{a}_{\mathrm{ex}}.\boldsymbol{b}') = \boldsymbol{a}_{\mathrm{ex}}.D\boldsymbol{b}' + \text{zeroth-order terms of } \boldsymbol{b}'.$$

The zeroth-order terms can then be included in the $\mathcal{O}(1, \boldsymbol{v})$ terms. Furthermore, we obtain first-derivative approximations of $\boldsymbol{v}'$, $\boldsymbol{p}'$ and $\boldsymbol{\rho}'$ in the pressure equation, but as in the continuous analysis, they are bounded by the corresponding principal terms, see Appendix A.1. Hence, the part of the scheme that affects the linear stability reduces to

$$\boldsymbol{\rho}_t' + \boldsymbol{\rho}_{\mathrm{ex}}.D\boldsymbol{v}' + \boldsymbol{v}_{\mathrm{ex}}.D\boldsymbol{\rho}' + hH^{-1}D_{(\delta)}^T\tilde{\Delta}D_{(\delta)}\boldsymbol{\rho}' = \mathcal{O}(1, \boldsymbol{v}),$$

$$\boldsymbol{v}_t' + \boldsymbol{v}_{\mathrm{ex}}.\tilde{D}\boldsymbol{v}' + \frac{1}{\boldsymbol{\rho}_{\mathrm{ex}}}.\tilde{D}\boldsymbol{p}' + hH^{-1}\tilde{D}_{(\delta)}^T\tilde{\Delta}D_{(\delta)}\boldsymbol{v}' = \frac{2\mu + \lambda}{\boldsymbol{\rho}_{\mathrm{ex}}}.\tilde{D}D\boldsymbol{v}' + \mathcal{O}(1, \boldsymbol{v}),$$

$$\boldsymbol{p}_t' + \boldsymbol{v}_{\mathrm{ex}}.D\boldsymbol{p}' + \gamma\boldsymbol{p}_{\mathrm{ex}}.D\boldsymbol{v}' + hH^{-1}D_{(\delta)}^T\tilde{\Delta}D_{(\delta)}\boldsymbol{p}' = (2\mu + \lambda)(\gamma - 1)(\overset{b,x}{\boldsymbol{v}}_{\mathrm{ex}} - \boldsymbol{v}_{\mathrm{ex}}).\tilde{D}D\boldsymbol{v}'$$

$$+ \frac{\kappa(\gamma-1)}{\mathcal{R}}\left(\frac{1}{\boldsymbol{\rho}_{\mathrm{ex}}}.DD\boldsymbol{p} - \frac{\boldsymbol{p}_{\mathrm{ex}}.}{\boldsymbol{\rho}_{\mathrm{ex}}.^2}.DD\boldsymbol{\rho}' - \frac{1}{\boldsymbol{\rho}_{\mathrm{ex}}}.H^{-1}BD\boldsymbol{p}'\right.$$

$$\left.+ \frac{\boldsymbol{p}_{\mathrm{ex}}.}{\boldsymbol{\rho}_{\mathrm{ex}}.^2}.H^{-1}BD\boldsymbol{\rho}'\right) + \mathcal{O}(1, \boldsymbol{v}).$$

In order to symmetrise the system, we must freeze the coefficients. That is, we assume that the variable coefficients are constants. Specifically, with $\boldsymbol{v}_{\mathrm{ex}} = constant$, the difference $(\overset{b,x}{\boldsymbol{v}}_{\mathrm{ex}} - \boldsymbol{v}_{\mathrm{ex}}) = 0$, since $\overset{b,x}{\boldsymbol{v}}_{\mathrm{ex}}$ is an arithmetic mean of $\boldsymbol{v}_{\mathrm{ex}}$. This would immediately take us to (16)-(18) (plus some benign terms), which we already know is stable. However, *the method of freezing the coefficients is only allowed if it implies stability of the variable-coefficient problems.*

Remark. Consider the advection equation, $u_t + a(x,t)u_x = 0$ whose estimate is $\partial_t \|u\|^2 + au^2|_0^1 + \int_0^1 a_x u^2 \, dx = 0$, and analogously for any SBP semi-discretisation. Clearly, if a bound is obtained for any constant a within the range of a, and $|a_x|$ is bounded, the variable-coefficient problem is also bounded.

Here, it is straightforward that the above principle applies to most terms. However, we can not immediately omit the term with $(\overset{b,x}{\boldsymbol{v}}_{\text{ex}} - \boldsymbol{v}_{\text{ex}})$ in the "freezing" process, since it is a part of a second-derivative term of velocity in the temperature equation. Hence, we keep it as a variable coefficient while all other coefficients are frozen (signified with the superscript star). By applying the symmetrising matrices from [1] and introducing $\hat{\boldsymbol{\rho}} = \frac{c^*}{\sqrt{\gamma}\rho^*}\rho'$ and $\hat{\text{T}} = -\frac{c^*}{\rho^*\sqrt{\gamma}\sqrt{\gamma-1}}\rho' + \sqrt{\frac{\gamma}{\gamma-1}}\frac{1}{\rho^*c^*}\boldsymbol{p}' = \frac{\gamma\mathcal{R}}{c^*\sqrt{\gamma}\sqrt{\gamma-1}}\text{T}'$ to reduce notation, we arrive at

$$\hat{\boldsymbol{\rho}}_t + v^* D\hat{\boldsymbol{\rho}} + \frac{c^*}{\sqrt{\gamma}}D\boldsymbol{v}' + hH^{-1}D_{(\delta)}^T \tilde{\Delta} D_{(\delta)}\hat{\boldsymbol{\rho}} = \mathcal{O}(1, \boldsymbol{v}), \tag{44}$$

$$\boldsymbol{v}'_t + \frac{c^*}{\sqrt{\gamma}}\tilde{D}\hat{\boldsymbol{\rho}} + v^*\tilde{D}\boldsymbol{v}' + \sqrt{\frac{\gamma-1}{\gamma}}c^*\tilde{D}\hat{\text{T}} + hH^{-1}\tilde{D}_{(\delta)}^T \tilde{\Delta} D_{(\delta)}\boldsymbol{v}' = \frac{2\mu+\lambda}{\rho^*}\tilde{D}D\boldsymbol{v}' + \mathcal{O}(1, \boldsymbol{v}), \tag{45}$$

$$\hat{\text{T}}_t + \sqrt{\frac{\gamma-1}{\gamma}}c^* D\boldsymbol{v}' + v^* D\hat{\text{T}} + hH^{-1}D_{(\delta)}^T \tilde{\Delta} D_{(\delta)}\hat{\text{T}} = \frac{\sqrt{\gamma}\sqrt{\gamma-1}}{\rho^*c^*}(2\mu+\lambda)(\overset{b,x}{\boldsymbol{v}}_{\text{ex}} - \boldsymbol{v}_{\text{ex}}).\tilde{D}D\boldsymbol{v}'$$
$$+ \frac{\gamma\mu}{\text{Pr}\rho^*}\left(DD\hat{\text{T}} - H^{-1}BD\hat{\text{T}}\right) + \mathcal{O}(1, \boldsymbol{v}). \tag{46}$$

Note the resemblance to (16)-(18).

Proposition 5.1. *The non-linear scheme* (43) *is linearly stable.*

Proof. Linearising and symmetrising the non-linear scheme (43) leads to (44)-(46). Linear stability can then be established by employing the discrete energy method. In this process, the terms that differ from the analysis in Proposition 4.1 are the artificial diffusion terms, the $\mathcal{O}(1, \boldsymbol{v})$-terms and the additional (velocity dependent) diffusive term in (46). The last one is the only non-trivial term. Hence, we only consider the temperature equation (the artificial diffusion terms and the $\mathcal{O}(1, \boldsymbol{v})$-terms are handled in the same way in (44) - (45)).

In the energy analysis for equation (46) we multiply by $\hat{\text{T}}^T H$ and add the transpose. We focus on the terms that differ from the scheme (18),

$$2h\hat{\text{T}}^T H H^{-1}D_{(\delta)}^T \tilde{\Delta} D_{(\delta)}\hat{\text{T}} - 2\frac{\sqrt{\gamma}\sqrt{\gamma-1}}{\rho^*c^*}(2\mu+\lambda)\hat{\text{T}}^T H\left((\overset{b,x}{\boldsymbol{v}}_{\text{ex}} - \boldsymbol{v}_{\text{ex}}).DD\boldsymbol{v}'\right) + 2\hat{\text{T}}^T H\mathcal{O}(1, \boldsymbol{v})$$

$$= 2h(D_{(\delta)}\hat{\text{T}})^T \tilde{\Delta} D_{(\delta)}\hat{\text{T}} + 2\frac{\sqrt{\gamma}\sqrt{\gamma-1}}{\rho^*c^*}(2\mu+\lambda)(D(\overset{b,x}{\boldsymbol{v}}_{\text{ex}} - \boldsymbol{v}_{\text{ex}}).\hat{\text{T}})^T H\left(D\boldsymbol{v}'\right) + 2\hat{\text{T}}^T H\mathcal{O}(1, \boldsymbol{v}). \tag{47}$$

The first term is quadratic with positive sign since $\tilde{\Delta}$ is diagonal and $\tilde{\Delta}_{ii} = \delta_{i+1/2} \geq 0$. Moreover, the last term will at most contribute with a finite growth in the final estimate. The only term that requires attention is: $(D(\overset{b,x}{\boldsymbol{v}}_{\text{ex}} - \boldsymbol{v}_{\text{ex}}).\hat{\text{T}})^T H(D\boldsymbol{v}')$. Since $\overset{b,x}{\boldsymbol{v}}_{\text{ex}}$ is an average of the smooth function $\boldsymbol{v}_{\text{ex}}$, $(\overset{b,x}{\boldsymbol{v}}_{\text{ex}} - \boldsymbol{v}_{\text{ex}}) \sim \mathcal{O}(h)$. Hence, $(D(\overset{b,x}{\boldsymbol{v}}_{\text{ex}} - \boldsymbol{v}_{\text{ex}}).\hat{\text{T}})^T H(D\boldsymbol{v}') \leq C\|D\hat{\text{T}}\|\|L(\boldsymbol{v}')\|$ where $L(\boldsymbol{v}')$ represents a vector whose entries are linear combinations of the elements of $\boldsymbol{v}'$. Hence, these terms do not cause an unbounded growth in the final estimate for all components. (They enter the estimate corresponding to (26) as $\|D\hat{\text{T}}\|^2$ and $\|\boldsymbol{v}'\|^2$ terms.) □

It is common to demonstrate linear stability of non-linear schemes by directly considering (16)-(18). Here, we have rigorously proven that the non-linear scheme (43) indeed reduces to (16)-(18).

Remark. A 3rd-order version of (43) is obtained as follows: Replace the difference operators D, with the diagonal-norm (4,2)-scheme that is 4th-order in the interior and 2nd-order near the boundaries, and $\tilde{D}$ with its counterpart obtained by zeroing the first and last row in the (4,2)-operator. (See [8] for information on the (4,2)-operator and [17] for high-order version of artificial diffusion.) We have verified the linearisation process for this scheme leading to (16)-(18) (now with the (4,2)-operators) and proven stability for the symmetrised scheme. (Note that the high-order scheme produce a different set of boundary terms in the energy estimate.)

5.2. Entropy

For the non-linear analysis, we give a brief summary of the theory of entropy and refer the reader to the papers of Harten ([10]) and Tadmor ([32]) for a more comprehensive introduction.

Hyperbolic conservation laws take the form

$$u_t + f(u)_x = 0, \qquad x \in \mathbb{R}. \tag{48}$$

A strictly convex scalar function, $U(u)$, is said to be an *entropy function* of the problem (48), if it satisfies the relation $U_u^T f_u = F_u$, where F is the entropy flux function. $U_u = w$ are the *entropy variables*, which symmetrises the problem (48) (see e.g. [12]). Furthermore, the scalar function $\psi = w^T f - F$ is called the entropy potential. By multiplying by the entropy variables, the equation (48) can be recast as

$$U(u)_t + F(u)_x = 0,$$

which is satisfied for smooth solutions of the problem (48). However, it is well-known that solutions of (48) can develop shocks (even from continuous data), and we therefore have to consider weak solutions that satisfy

$$\int_{\mathbb{R}} \phi u_t \, dx - \int_{\mathbb{R}} \phi_x f(u) \, dx = 0,$$

for any $\phi \in \mathcal{C}^\infty$ with compact support. Weak solutions are generally not unique, however, the physically relevant solution satisfies the Second Law of Thermodynamics, which states that the entropy within a closed system cannot decrease. In mathematical terms, this can be stated as the entropy inequality

$$U(u)_t + F(u)_x \leq 0. \tag{49}$$

Solutions that satisfy the *entropy inequality* (49) are called *entropy solutions* (see e.g. [32]).

5.3. Entropy stability

In order to carry the concept of entropy over to the semi-discrete setting, we consider a scheme of the form

$$(u_i)_t + \frac{g_{i+1/2} - g_{i-1/2}}{h_i} = 0, \tag{50}$$

where h_i is the distance between grid node $i+1$ and i. Furthermore, $g_{i+1/2} = \frac{f_{i+1} + f_i - \delta_{i+1/2}(u_{i+1} - u_i)}{2}$ is the approximation of the flux $f(u)$, where $\delta_{i+1/2}(u_{i+1} - u_i)$, with $\delta_{i+1/2} \geq 0$, is an artificial dissipation term. Schemes such as (50) are termed entropy stable, if they satisfy the discrete entropy inequality

$$(U_i)_t + \frac{F_{i+1/2} - F_{i-1/2}}{h_i} \leq 0, \quad \text{for all } i, \tag{51}$$

where $F_{i+1/2} = \frac{1}{2}\left((\boldsymbol{w}_{i+1}^T + \boldsymbol{w}_i^T)g_{i+1/2}\right) - \frac{1}{2}(\psi_{i+1} + \psi_i)$, and $\psi_i = \psi(u_i)$. This holds true for schemes where δ is chosen such that the flux approximation satisfies *Tadmor's shuffle condition*,

$$\langle \Delta w_{i+1/2}, g_{i+1/2} \rangle \leq \Delta \psi_{i+1/2} = \psi_{i+1} - \psi_i, \tag{52}$$

where $\Delta w_{i+1/2} = w_{i+1} - w_i$. See [32] for more details.

5.4. Entropy analysis for the 1-D Navier-Stokes equations

Consider the continuous problem (10) augmented with the no-slip wall boundary condition $v(0, t) = 0$, and a Neumann condition on the temperature; $T_x(0, t) = 0$ (neglecting the right boundary), and L^2-bounded initial data. (The entropy estimate for this problem is derived in e.g. [23] and also [31], but we repeat it here for completeness.)

For the compressible Navier-Stokes equations, there is only one entropy function ([11]); $U(u) = -\rho S$ with $F(u) = -mS$ and $\psi = (\gamma - 1)m$, where $S = \ln\left(\frac{p}{\rho^\gamma}\right)$, and S is the specific entropy. For this entropy function, the entropy variables are given by

$$w^T = -\frac{1}{c_v T}\left(\frac{v^2}{2} + c_v T(S - \gamma), -v, 1\right).$$

To obtain an entropy estimate, multiply Equation (10) by the entropy variables, w^T, and integrate over the spatial domain $\Omega = (0, 1)$,

$$\int_\Omega U(u)_t \, dx + \int_\Omega F(u)_x \, dx = \int_\Omega w^T f^v(u, u_x)_x \, dx,$$

which leads to

$$\int_\Omega U(u)_t \, dx - F(u)|_0 = -w^T f^v(u, u_x)|_0 - \int_\Omega w_x^T f^v(u, u_x) \, dx.$$

Since $F = -m\mathcal{S}$, we have that $F(u)|_0 = 0$, due to the no-slip boundary condition. Furthermore, the term $w^T f^v(u, u_x)|_0$ reduces to

$$w^T f^v(u, u_x)\big|_0 = -\frac{(\gamma - 1)\kappa}{\mathcal{R}} \frac{T_x}{T}\bigg|_0 = 0,$$

(see e.g. [23]). The last equality is due to the Neumann condition at $x = 0$. Hence, the estimate reads

$$\int_\Omega U(u)_t \, dx = -\int_\Omega \frac{1}{c_v T^2}\left((2\mu + \lambda)v_x^2 T + \kappa T_x^2\right) dx. \tag{53}$$

Since admissible solutions satisfy $T > 0$, the entropy is bounded from above.

5.4.1. Non-linear stability

We now turn to the non-linear analysis of the scheme (27), and show that it is entropy stable.

Proposition 5.2. *If* f^I *satisfies* (52) *for* $i = 1, \ldots, N - 1$, *then the semi-discrete scheme* (27)

$$u_t + \mathcal{D}^I f^I = \mathcal{D}^v f^v + \mathsf{SAT}, \tag{27}$$

with (28)-(34), *approximating system* (10) *is entropy-stable in the sense of* (51).

Remark. The scheme (27) is inspired by the one proposed in [31] and [25].

Remark. Possible entropy stable choices of f^I are for instance the local- and global Lax-Friedrichs schemes and entropy-fixed Roe schemes. An entropy conservative flux can be recast into the form of (29). For linear stability, it is evident that we need $\delta_{i+1/2} \geq 0$ for all i, (cf. (47)) which is not necessarily true for entropy *conservative* fluxes (see [6]). However, the non-linear analysis presented below holds also for entropy conservative fluxes.

Proof. For each grid point, multiply the scheme (27) by the corresponding entropy variable $w_i^T = -\frac{1}{c_v T_i}\left(\frac{v_i^2}{2} + c_v T_i(\mathcal{S}_i - \gamma)\right)$, $-v_i, 1$) and the norm element H_{ii} (the i-th diagonal element of H), and sum over all nodes (and neglect the right boundary for brevity)

$$\sum_{i=0}^{N-1} w_i^T H_{ii}(u_i)_t + \sum_{i=0}^{N-1} w_i^T H_{ii}(\mathcal{D}^I f^I)_i = \sum_{i=0}^{N-1} w_i^T H_{ii}(\mathcal{D}^v f^v)_i + \sum_{i=0}^{N-1} w_i^T H_{ii}\mathsf{SAT}_i. \tag{54}$$

For the convective flux approximation, we perform the analysis using index notation in order to use the entropy stability results in [32]. The left-hand side of (54) is recast as

$$\sum_{i=0}^{N-1} w_i^T H_{ii}(u_i)_t + \sum_{i=0}^{N-1} w_i^T H_{ii}(\mathcal{D}^I f^I)_i = \sum_{i=0}^{N-1} H_{ii}(U_i)_t + \underbrace{w_0^T H_{00}(\mathcal{D}^I f^I)_0 + \sum_{i=1}^{N-1} w_i^T H_{ii}\left(\mathcal{D}^I f^I\right)_i}_{A}. \tag{55}$$

Utilising (28) and the theory of [32], we manipulate A as

$$A = w_0^T H_{00}(\mathcal{D}^I f^I)_0 - \sum_{i=1}^{N-1} F_{i-1/2} + \sum_{i=1}^{N-1} F_{i+1/2}$$

$$- \sum_{i=1}^{N-1}\left(\frac{1}{2}(w_i - w_{i-1})^T f^I_{i-1/2} - \frac{1}{2}(\psi_i - \psi_{i-1})\right) - \sum_{i=1}^{N-1}\left(\frac{1}{2}(w_{i+1} - w_i)^T f^I_{i+1/2} - \frac{1}{2}(\psi_{i+1} - \psi_i)\right),$$

where $F_{i+1/2} = \frac{w_{i+1}^T + w_i^T}{2}f^I_{i+1/2} - \frac{\psi_{i+1} + \psi_i}{2}$. All F's except $F_{1/2}$ cancel due to the series' telescoping nature. Assuming that Tadmor's shuffle condition (52) is fulfilled, A reduces to

$$A \geq w_0^T H_{00}(\mathcal{D}^I f^I)_0 - F_{1/2} = w_0^T H_{00}\frac{f^I_{1/2} - f^I_0}{h/2} - F_{1/2} = w_0^T(f^I_{1/2} - f^I_0) - F_{1/2} \geq -w_0^T f^I_0 + \psi_0,$$

where we in the last step have used similar manipulations as for the interior nodes. Thanks to $v_0 = 0$, the entropy variable corresponding to the momentum equation is $w_0^m = \frac{v_0}{c_v T_0} = 0$, $\psi = (\gamma - 1)(\rho.v)_0 = 0$ and by (30) and (32), $f_0^{I,\rho} = (\rho.v)_0 = 0$ and $f_0^{I,E} = (v.(E + p))_0 = 0$ respectively, such that we obtain $A \geq 0$. Equation (54) therefore reduces to

$$\sum_{i=0}^{N} H_{ii}(U_i)_t \leq \sum_{i=0}^{N} \boldsymbol{w}_i^T H_{ii}(\mathcal{D}^{\vee}\mathbf{f}^{\vee})_i + \sum_{i=0}^{N} \boldsymbol{w}_i^T H_{ii}\mathsf{SAT}_i. \tag{56}$$

For the analysis of the diffusive term, we introduce the following vectors

$$
\begin{aligned}
\boldsymbol{w}^m &= \begin{pmatrix} w_0^m, & w_1^m, & w_2^m, & \ldots, & w_N^m \end{pmatrix}^T = \begin{pmatrix} \frac{v_0}{c_v T_0}, & \frac{v_1}{c_v T_1}, & \frac{v_2}{c_v T_2}, & \ldots, & \frac{v_N}{c_v T_N} \end{pmatrix}^T, \\
\boldsymbol{w}^E &= \begin{pmatrix} w_0^E, & w_1^E, & w_2^E, & \ldots, & w_N^E \end{pmatrix}^T = \begin{pmatrix} -\frac{1}{c_v T_0}, & -\frac{1}{c_v T_1}, & -\frac{1}{c_v T_2}, & \ldots, & -\frac{1}{c_v T_N} \end{pmatrix}^T,
\end{aligned}
\tag{57}
$$

where the superscript denotes which equation the vector acts on. Using (33) and (34) the right-hand side of (56) can be restated using matrix notation as

$$
\begin{aligned}
\sum_{i=0}^{N-1} \left(\boldsymbol{w}_i^T H_{ii}(\mathcal{D}^{\vee}\mathbf{f}^{\vee})_i + \boldsymbol{w}_i^T H_{ii}\mathsf{SAT} \right) &= \underbrace{(\boldsymbol{w}^m)^T H\tilde{D}\left((2\mu+\lambda)D\boldsymbol{v}\right)}_{A_1} \\
&\quad + \underbrace{(\boldsymbol{w}^E)^T H\left(D\left((2\mu+\lambda)\overset{b,x}{\boldsymbol{v}}.D\boldsymbol{v}+\kappa D\mathsf{T}\right) - \kappa H^{-1}BD\mathsf{T}\right)}_{A_2}.
\end{aligned}
\tag{58}
$$

Utilising that $H\tilde{D} = \tilde{Q} = \tilde{B} - \tilde{Q}^T = \tilde{B} - (H\tilde{D})^T$ and (15) we obtain

$$
\begin{aligned}
A_1 &= (2\mu+\lambda)(\boldsymbol{w}^m)^T \tilde{B}D\boldsymbol{v} - (2\mu+\lambda)(\tilde{D}\boldsymbol{w}^m)^T HD\boldsymbol{v} \\
&= -\frac{(2\mu+\lambda)}{2}\left(w_1^m(D\boldsymbol{v})_0 + w_0^m(D\boldsymbol{v})_1\right) - (2\mu+\lambda)(\tilde{D}\boldsymbol{w}^m)^T HD\boldsymbol{v}.
\end{aligned}
$$

Insert $w_1^m = \frac{v_1}{c_v T_1}$ and $v_0 = 0$ to obtain

$$
\begin{aligned}
A_1 &= -\frac{(2\mu+\lambda)}{2h}\frac{1}{c_v T_1}v_1(v_1-v_0) - (2\mu+\lambda)(\tilde{D}\boldsymbol{w}^m)^T HD\boldsymbol{v}, \\
&= -\frac{(2\mu+\lambda)}{2h}\frac{1}{c_v T_1}v_1^2 - (2\mu+\lambda)(\tilde{D}\boldsymbol{w}^m)^T HD\boldsymbol{v} \leq -(2\mu+\lambda)(\tilde{D}\boldsymbol{w}^m)^T HD\boldsymbol{v}.
\end{aligned}
\tag{59}
$$

Next, we turn to A_2 on the right-hand side of equation (58). Utilising the SBP properties, $HD = Q$ and $Q = B - Q^T$ yields

$$
\begin{aligned}
A_2 &= (\boldsymbol{w}^E)^T B\left((2\mu+\lambda)\overset{b,x}{\boldsymbol{v}}.D\boldsymbol{v}+\kappa D\mathsf{T}\right) - \kappa(\boldsymbol{w}^E)^T BD\mathsf{T} - (\boldsymbol{w}^E)^T Q^T\left((2\mu+\lambda)\overset{b,x}{\boldsymbol{v}}.D\boldsymbol{v}+\kappa D\mathsf{T}\right), \\
&= -(D\boldsymbol{w}^E)^T H\left((2\mu+\lambda)\overset{b,x}{\boldsymbol{v}}.D\boldsymbol{v}+\kappa D\mathsf{T}\right),
\end{aligned}
\tag{60}
$$

where we used $\overset{b,x}{v}_0 = v_0 = 0$ in the last step.

Combining the preliminary results (56), (59) and (60) leads to

$$
\sum_{i=0}^{N} H_{ii}(U_i)_t \leq -(2\mu+\lambda)\underbrace{\left((\tilde{D}\boldsymbol{w}^m)^T HD\boldsymbol{v} + (D\boldsymbol{w}^E)^T H(\overset{b,x}{\boldsymbol{v}}.D\boldsymbol{v})\right)}_{A_3} - \underbrace{\kappa(D\boldsymbol{w}^E)^T HD\mathsf{T}}_{A_4}.
$$

Using (57) and the discrete product rule (39) result in

$$
\begin{aligned}
A_3 &= \frac{1}{c_v}\left(\tilde{D}(\boldsymbol{v}.\mathsf{T}^{-1})\right)^T HD\boldsymbol{v} - \frac{1}{c_v}\left(D\mathsf{T}^{-1}\right)^T H(\overset{b,x}{\boldsymbol{v}}.D\boldsymbol{v}), \\
&= \frac{1}{c_v}\left(\left(\overset{i,x}{\mathsf{T}^{-1}}.\tilde{D}\boldsymbol{v}\right)^T HD\boldsymbol{v} + \left(\overset{b,x}{\boldsymbol{v}}.\tilde{D}\mathsf{T}^{-1}\right)^T HD\boldsymbol{v} - \left(D\mathsf{T}^{-1}\right)^T H(\overset{b,x}{\boldsymbol{v}}.D\boldsymbol{v})\right).
\end{aligned}
$$

The first term in the last row is a discrete equivalent of the L^2-norm, $\left(\overset{i,x}{\mathsf{T}^{-1}}.\tilde{D}\boldsymbol{v}\right)^T HD\boldsymbol{v} = \sum_{i=0}^{N}(\overset{i,x}{\mathsf{T}^{-1}})_i(\tilde{D}\boldsymbol{v})_i H_{ii}(D\boldsymbol{v})_i =$

$\|\sqrt{\overset{i,x}{\mathsf{T}^{-1}}}.\tilde{D}\boldsymbol{v}\|_H^2 \geq 0$, $(\mathsf{T} > 0)$. (Note that $(\tilde{D}\boldsymbol{v})_0(D\boldsymbol{v})_0 = (\tilde{D}\boldsymbol{v})_0^2 = 0$.) Furthermore, it is easily verified that the two last terms cancel.

Lastly, by the discrete quotient rule (40), we have

$$A_4 = \kappa (D\mathbf{w}^E)^T H D \mathrm{T} = -\frac{1}{c_v}\kappa \left(D\mathrm{T}^{-1}\right)^T H D \mathrm{T} = \frac{\kappa (\overset{x}{\mathrm{T}^2})^{-1}}{c_v} \cdot (D\mathrm{T})^T H D \mathrm{T} = \frac{\kappa}{c_v}\|\sqrt{(\overset{x}{\mathrm{T}^2})^{-1}}.D\mathrm{T}\|_H^2,$$

where $(\overset{x}{\mathrm{T}})_0^2 = \mathrm{T}_0 \mathrm{T}_1$ and $(\overset{x}{\mathrm{T}})_i^2 = \mathrm{T}_{i-1}\mathrm{T}_{i+1}$, $i = 1, \dots, N-1$. This term is non-negative as long as all T_i's > 0.

Finally, our entropy estimate (54) reads

$$\sum_{i=0}^N H_{ii}(U_i)_t \le -(2\mu + \lambda)\|\sqrt{\overset{i,x}{\mathrm{T}^{-1}}}.\tilde{D}\mathbf{v}\|_H^2 - \frac{\kappa}{c_v}\|\sqrt{(\overset{x}{\mathrm{T}^2})^{-1}}.D\mathrm{T}\|_H^2 \le 0.$$

Hence, we conclude that our scheme is entropy stable. □

5.5. Non-linear analysis for the 2-D Navier-Stokes equations

Let $\Omega = (0,1) \times (0,1)$ be the spatial domain with boundary $\partial\Omega$. The compressible Navier-Stokes equations in two space dimensions are stated as

$$u_t + f_x^I + g_y^I = f^v(u, u_x, u_y)_x + g^v(u, u_x, u_y)_y, \quad (x,y) \in \Omega = (0,1)^2, \quad 0 < t < \mathcal{T}, \tag{61}$$

where $u = (\rho, m, n, E)^T$ are the conserved variables and

$$f^I = \left(m, \rho v_1^2 + p, \rho v_1 v_2, v_1(E+p)\right)^T,$$
$$g^I = \left(n, \rho v_1 v_2, \rho v_2^2 + p, v_2(E+p)\right)^T,$$
$$f^v = \left(0, 2\mu v_{1_x} + \lambda\left(v_{1_x} + v_{2_y}\right), \mu\left(v_{1_y} + v_{2_x}\right), v_1\left(2\mu v_{1_x} + \lambda\left(v_{1_x} + v_{2_y}\right)\right) + \mu v\left(v_{1_y} + v_{2_x}\right) + \kappa \mathrm{T}_x\right)^T,$$
$$g^v = \left(0, \mu\left(v_{1_y} + v_{2_x}\right), 2\mu v_{2_y} + \lambda\left(v_{1_x} + v_{2_y}\right), v_2\left(2\mu v_{2_y} + \lambda\left(v_{1_x} + v_{2_y}\right)\right) + \mu v_1\left(v_{1_y} + v_{2_x}\right) + \kappa \mathrm{T}_y\right)^T,$$

are the inviscid and viscous fluxes; $n = \rho v_2$ is the momentum in the y-direction and v_1, v_2 denote the velocity components in the x- and y-directions, respectively. Equation (61) is augmented with no-slip boundary conditions and homogeneous Neumann conditions for the temperature, i.e.

$$v_1|_{\partial\Omega} = 0, \quad v_2|_{\partial\Omega} = 0, \quad \frac{\partial \mathrm{T}}{\partial n}|_{\partial\Omega} = 0, \tag{62}$$

and appropriate initial conditions. In 2-D, the entropy fluxes are $F_x = w^T f_x^I$ and $G_y = w^T g_y^I$, where $F = -m\mathcal{S}$ and $G = -n\mathcal{S}$. Following the same procedure as for the one-dimensional case, we can demonstrate that this problem satisfies the entropy inequality (49) (see again [23] or [31] for the derivation in 3-D). That is, multiply equation (61) by the entropy variables $w^T = -\frac{1}{c_v \mathrm{T}}\left(\frac{v_1^2 + v_2^2}{2} + c_v \mathrm{T}(\mathcal{S} - \gamma), -v_1, -v_2, 1\right)$ and integrate over the spatial domain. Apply integration-by-parts to the entropy flux function and the viscous flux. Ignoring the boundaries at $x = 1$ and $y = 1$, this results in

$$\int_\Omega U_t \, d\Omega - \int_{\partial\Omega, x=0} F \, dy - \int_{\partial\Omega, y=0} G \, dx = -\int_{\partial\Omega, x=0} w^T f^v \, dy - \int_{\partial\Omega, y=0} w^T g^v \, dx - \int_\Omega w_x^T f^v + w_y^T g^v \, d\Omega.$$

In view of (62), $F = G = 0$ at the boundaries. Using the temperature condition in (62), the boundary integrals take the form

$$\int_{\partial\Omega, x=0} w^T f^v \, dy = -\frac{\kappa}{c_v} \int_{\partial\Omega, x=0} \frac{\mathrm{T}_x}{\mathrm{T}} \, dy = 0, \quad \int_{\partial\Omega, y=0} w^T g^v \, dx = -\frac{\kappa}{c_v} \int_{\partial\Omega, y=0} \frac{\mathrm{T}_y}{\mathrm{T}} \, dx = 0.$$

Furthermore, by contracting the derivatives of the entropy variables with f^v and g^v, and using $\lambda = -\frac{2}{3}\mu$ we obtain

$$w_x^T f^v + w_y^T g^v = \frac{1}{c_v \mathrm{T}}\left(\frac{2}{3}\mu\left(v_{1_x} - v_{2_y}\right)^2 + \frac{2}{3}\mu v_{1_x}^2 + \frac{2}{3}\mu v_{2_y}^2 + \mu\left(v_{1_y} + v_{2_x}\right)^2\right) + \frac{\kappa}{c_v}\frac{\mathrm{T}_x^2 + \mathrm{T}_y^2}{\mathrm{T}^2} \ge 0,$$

as long as $\mathrm{T} > 0$. Hence, we have proved that $\int_\Omega U_t \, d\Omega \le 0$.

5.6. Entropy stability for the semi-discrete scheme

For the discretisation in two spatial dimensions, we use the formalism found in e.g. [29]. We divide the spatial domain into $(N+1)(M+1)$ grid points, such that $x_i = ih_x$, $i = 0, 1, \ldots N$, where $h_x = 1/N$ and $y_i = ih_y$, $i = 0, 1, \ldots, M$ where $h_y = 1/M$. We denote $u_{i,j}(t)$ as the approximation of $u(x_i, y_j, t)$, and the solution vectors are ordered in the following way

$$\boldsymbol{u}^T = (u_{0,0}, u_{1,0}, \ldots, u_{N,0}, u_{0,1}, u_{1,1}, \ldots, u_{N,1}, \ldots, u_{0,M}, u_{1,M}, \ldots, u_{N,M}).$$

The 2-D differential operators are defined by Kronecker products as $D_x = I_M \otimes D_N$, where I_M is the $(M+1) \times (M+1)$ identity matrix, and D_N is the $(N+1) \times (N+1)$ (2,1)-SBP operator. Similarly, we have $D_y = D_M \otimes I_N$.

To impose the no-slip boundary conditions by injection, we introduce the initial velocity solution vectors as

$$(\boldsymbol{v}^1)^T = (0, 0, 0, \ldots, 0, 0, v^1_{1,1}, v^1_{2,1}, \ldots, 0, 0, v^1_{1,M-1}, v^1_{2,M-1}, \ldots, v^1_{N,M-1}, 0, 0, 0, \ldots, 0),$$
$$(\boldsymbol{v}^2)^T = (0, 0, 0, \ldots, 0, 0, v^2_{1,1}, v^2_{2,1}, \ldots, 0, 0, v^2_{1,M-1}, v^2_{2,M-1}, \ldots, v^2_{N,M-1}, 0, 0, 0, \ldots, 0),$$

i.e., $\boldsymbol{v}^1$ and $\boldsymbol{v}^2$ have all elements along $x = 0$, $x = 1$, $y = 0$ and $y = 1$ set to zero. In addition, we define the SBP-operators for the momentum equations so that they do not act on the boundary nodes.

$$\tilde{D}_x = (\tilde{I}_M \otimes \tilde{D}_N), \quad \tilde{D}_y = (\tilde{D}_M \otimes \tilde{I}_N),$$

where $\tilde{D}_N$ and $\tilde{D}_M$ are Dirichlet-SBP operators corresponding to D_N and D_M, respectively. Moreover, $\tilde{I}_N$ and $\tilde{I}_M$ are almost the identity matrices, but with the upper left and lower right elements set to zero. The norm matrix for the two-dimensional grid is given by $H = H_y \otimes H_x$, where H_y and H_x are equal to the 1-D norms defined in Section 3, with elements of size h_y and h_x and matrix sizes $(M+1) \times (M+1)$ and $(N+1) \times (N+1)$, respectively.

Similarly as for the one-dimensional case, the SBP operators satisfy a discrete product - (39) and quotient (40) rule.

5.7. Entropy stability for the semi-discrete scheme

The 2-D inviscid fluxes are approximated by

$$\boldsymbol{f}^\mathsf{I}_{i+1/2,j} = \frac{\boldsymbol{f}^\mathsf{I}_{i+1,j} + \boldsymbol{f}^\mathsf{I}_{i,j}}{2} - \frac{\delta_{i+1/2,j}\left(\boldsymbol{u}_{i+1,j} - \boldsymbol{u}_{i,j}\right)}{2},$$
$$\boldsymbol{g}^\mathsf{I}_{i,j+1/2} = \frac{\boldsymbol{g}^\mathsf{I}_{i,j+1} + \boldsymbol{g}^\mathsf{I}_{i,j}}{2} - \frac{\delta_{i,j+1/2}\left(\boldsymbol{u}_{i,j+1} - \boldsymbol{u}_{i,j}\right)}{2},$$

and the convective terms by the flux differences

$$\begin{aligned}
(\mathcal{D}^\mathsf{I}_x \boldsymbol{f}^\mathsf{I})_{i,j} &= \frac{\boldsymbol{f}^\mathsf{I}_{i+1/2,j} - \boldsymbol{f}^\mathsf{I}_{i-1/2,j}}{h_x}, \quad i = 1, \ldots, N-1, \quad j = 0, \ldots, M, \\
(\mathcal{D}^\mathsf{I}_y \boldsymbol{g}^\mathsf{I})_{i,j} &= \frac{\boldsymbol{g}^\mathsf{I}_{i,j+1/2} - \boldsymbol{g}^\mathsf{I}_{i,j-1/2}}{h_y}, \quad i = 0, \ldots, N, \quad j = 1, \ldots, M-1,
\end{aligned} \tag{63}$$

in the interior and by

$$\begin{aligned}
(\mathcal{D}^\mathsf{I}_x \boldsymbol{f}^\mathsf{I})_{0,j} &= \frac{\boldsymbol{f}^\mathsf{I}_{1/2,j} - \boldsymbol{f}^\mathsf{I}_{0,j}}{h_x/2}, \quad i = 0, \quad j = 0, \ldots, M, \\
(\mathcal{D}^\mathsf{I}_y \boldsymbol{g}^\mathsf{I})_{i,0} &= \frac{\boldsymbol{g}^\mathsf{I}_{i,1/2} - \boldsymbol{g}^\mathsf{I}_{i,0}}{h_y/2}, \quad i = 0, \ldots, N, \quad j = 0,
\end{aligned} \tag{64}$$

at the boundaries $x = 0$, $y = 0$ (once again, we neglect the right and upper boundaries to reduce notation). As in the 1-D case, we have

$$\boldsymbol{f}^{\mathsf{I},\rho}_{0,j} = (\boldsymbol{\rho}.\boldsymbol{v}^1)_{0,j}, \quad \boldsymbol{f}^{\mathsf{I},m}_{0,j} = \boldsymbol{f}^{\mathsf{I},m}_{1/2,j}, \quad \boldsymbol{f}^{\mathsf{I},n}_{0,j} = \boldsymbol{f}^{\mathsf{I},n}_{1/2,j}, \quad \boldsymbol{f}^{\mathsf{I},E}_{0,j} = (\boldsymbol{v}^1.(\boldsymbol{E} + \boldsymbol{p}))_{0,j},$$

and similarly for $\boldsymbol{g}^\mathsf{I}_{i,0}$.

Next, we approximate the viscous terms by

$$\mathcal{D}^\mathsf{v}_x \boldsymbol{f}^\mu = \begin{pmatrix} 0 \\ \tilde{D}_x\left(\mathbf{1}_{\boldsymbol{x}}.\left(2\mu D_x \boldsymbol{v}^1 + \lambda(D_x \boldsymbol{v}^1 + D_y \boldsymbol{v}^2)\right)\right) \\ \tilde{D}_x\left(\mathbf{1}_{\boldsymbol{x}}.\left(\mu(D_y \boldsymbol{v}^1 + D_x \boldsymbol{v}^2)\right)\right) \\ D_x\left(\mathbf{1}_{\boldsymbol{x}}.\left(\overset{b,x}{\boldsymbol{v}^1}\left(2\mu D_x \boldsymbol{v}^1 + \lambda(D_x \boldsymbol{v}^1 + D_y \boldsymbol{v}^2)\right) + \mu \overset{b,x}{\boldsymbol{v}^2}(D_y \boldsymbol{v}^1 + D_x \boldsymbol{v}^2)\right)\right) \end{pmatrix}, \tag{65}$$

$$\mathcal{D}_y^{\vee} \mathbf{g}^{\mu} = \begin{pmatrix} 0 \\ \tilde{D}_y \left(\mathbf{1}_{\boldsymbol{y}} . \left(\mu(D_y \boldsymbol{v}^1 + D_x \boldsymbol{v}^2) \right) \right) \\ \tilde{D}_y \left(\mathbf{1}_{\boldsymbol{y}} . \left(2\mu D_y \boldsymbol{v}^2 + \lambda(D_x \boldsymbol{v}^1 + D_y \boldsymbol{v}^2) \right) \right) \\ D_y \left(\mathbf{1}_{\boldsymbol{y}} . \left(\overset{b,y}{\boldsymbol{v}^2} \left(2\mu D_y \boldsymbol{v}^2 + \lambda(D_x \boldsymbol{v}^1 + D_y \boldsymbol{v}^2) \right) + \mu \overset{b,y}{\boldsymbol{v}^1} (D_y \boldsymbol{v}^1 + D_x \boldsymbol{v}^2) \right) \right) \end{pmatrix}, \tag{66}$$

where we have used the approximation of 1 from [31]:

$$[\mathbf{1}_{\boldsymbol{x}}]_{i,j} = \frac{\mathrm{T}_{i,j}^{-1}}{\overset{i,x}{\mathrm{T}^{-1}_{i,j}}}, \qquad [\mathbf{1}_{\boldsymbol{y}}]_{i,j} = \frac{\mathrm{T}_{i,j}^{-1}}{\overset{i,y}{\mathrm{T}^{-1}_{i,j}}}. \tag{67}$$

Note that the operator $\mathcal{D}_{x,y}$ uses $\tilde{D}_{x,y}$ for the momentum equations where the no-slip condition is imposed by injection, and uses $D_{x,y}$ for the continuity equation and the equation for total energy.

Lastly, the approximations of the heat diffusive fluxes are given by

$$\mathcal{D}_x^{\vee} \mathbf{f}^{\kappa} = \left(0, 0, 0, \kappa D_x D_x \mathrm{T} \right)^T, \quad \mathcal{D}_y^{\vee} \mathbf{g}^{\kappa} = \left(0, 0, 0, \kappa D_y D_y \mathrm{T} \right)^T. \tag{68}$$

Then, a semi-discretisation of (61) is given by

$$\mathbf{u}_t + \mathcal{D}_x^{\mathsf{I}} \mathbf{f}^{\mathsf{I}} + \mathcal{D}_y^{\mathsf{I}} \mathbf{g}^{\mathsf{I}} = \mathcal{D}_x^{\vee} \mathbf{f}^{\mu} + \mathcal{D}_x^{\vee} \mathbf{f}^{\kappa} + \mathcal{D}_y^{\vee} \mathbf{g}^{\mu} + \mathcal{D}_y^{\vee} \mathbf{g}^{\kappa} + \mathsf{SAT}, \tag{69}$$

with $\mathsf{SAT} = \left(0, 0, 0, -\kappa \left((I_M \otimes H_x^{-1} B)(D_x \mathrm{T} - 0) + (H_y^{-1} B \otimes I_N)(D_y \mathrm{T} - 0) \right) \right)^T$.

Remark. Our scheme resembles the ones proposed in [31], where the no-slip condition was imposed using SAT, and [25].

Proposition 5.3. *The 2D semi-discrete scheme* (69) *approximating the problem* (61) *is entropy stable.*

Before stating the proof, we prove several lemmas to simplify the presentation. Similarly as in the proof of Proposition (5.2), we perform the calculations for the convective terms using index notation. To this end, we define $\boldsymbol{w}_{i,j}^T = \frac{1}{c_v \mathrm{T}_{i,j}} \left(\frac{(v_{i,j}^1)^2 + (v_{i,j}^2)^2}{2} + c_v \mathrm{T}_{i,j}(\mathcal{S}_{i,j} - \gamma), -v_{i,j}^1, -v_{i,j}^2, 1 \right).$

Lemma 5.4. *The convective flux approximations* (63) *and* (64) *satisfy*

$$\sum_{i,j=0}^{N,M} \boldsymbol{w}_{i,j}^T H_k(\mathcal{D}_x^{\mathsf{I}} \mathbf{f}^{\mathsf{I}})_{i,j} + \sum_{i,j=0}^{N,M} \boldsymbol{w}_{i,j}^T H_k(\mathcal{D}_y^{\mathsf{I}} \mathbf{g}^{\mathsf{I}})_{i,j} \geq 0, \tag{70}$$

(where $k = (j(N+1) + i)$ and H_k denotes the diagonal elements of H).

Proof. (70) follows by applying the same technique as for A in (55) to all j's in the x-direction for $\mathbf{f}^{\mathsf{I}}$ and to all i's in the y-direction for $\mathbf{g}^{\mathsf{I}}$. $\square$

For the diffusive terms, we define $\mathbf{H} = \mathrm{diag}(H, H, H, H)^T$ and $\boldsymbol{w}^T = \left((\boldsymbol{w}^{\rho})^T, (\boldsymbol{w}^m)^T, (\boldsymbol{w}^n)^T, (\boldsymbol{w}^E)^T \right)^T$ where

$$\begin{aligned} \boldsymbol{w}^{\rho} &= \frac{1}{c_v} \mathrm{T}^{-1} . \left(\frac{\boldsymbol{v}^1 . \boldsymbol{v}^1 + \boldsymbol{v}^2 . \boldsymbol{v}^2}{2} + c_v \mathrm{T} . (\mathcal{S} - \gamma) \right), \\ \boldsymbol{w}^m &= -\frac{1}{c_v} \mathrm{T}^{-1} . \boldsymbol{v}^1, \\ \boldsymbol{w}^n &= -\frac{1}{c_v} \mathrm{T}^{-1} . \boldsymbol{v}^2, \\ \boldsymbol{w}^E &= \frac{1}{c_v} \mathrm{T}^{-1}, \end{aligned} \tag{71}$$

and $[\mathrm{T}^{-1}]_{i,j} = \frac{1}{\mathrm{T}_{i,j}}$. (Recall that the dot product is the component wise vector multiplication.)

Lemma 5.5. *Contracting the entropy variables with the viscous fluxes, we obtain*

$$\boldsymbol{w}^T \mathbf{H}(\mathcal{D}_x^{\vee} \mathbf{f}^{\mu} + \mathcal{D}_y^{\vee} \mathbf{g}^{\mu}) \leq 0. \tag{72}$$

Proof. Consider the viscous flux in the x-direction given by (65). Contracting the vector (65) by the entropy variables in (71) and $\mathbf{H}$, we obtain

$$
\begin{aligned}
A_1 &= \mathbf{w}^T \mathbf{H} \mathcal{D}_x^v \mathbf{f}^\mu, \\
&= (\mathbf{w}^m)^T H \tilde{D}_x \big(\mathbf{1}_x. \big(2\mu D_x \mathbf{v}^1 + \lambda(D_x \mathbf{v}^1 + D_y \mathbf{v}^2)\big)\big) + (\mathbf{w}^n)^T H \tilde{D}_x \big(\mathbf{1}_x. \big(\mu(D_y \mathbf{v}^1 + D_x \mathbf{v}^2)\big)\big) \\
&\quad + (\mathbf{w}^E)^T H D_x \big(\mathbf{1}_x. \big(\overset{b,x}{\mathbf{v}^1}. \big(2\mu D_x \mathbf{v}^1 + \lambda(D_x \mathbf{v}^1 + D_y \mathbf{v}^2)\big) + \mu \overset{b,x}{\mathbf{v}^2}.(D_y \mathbf{v}^1 + D_x \mathbf{v}^2)\big)\big).
\end{aligned}
$$

Utilise that $H\tilde{D}_x = \tilde{H}_y \otimes \tilde{B}_N - \tilde{H}_y \otimes (H_x \tilde{D}_N)^T = \tilde{H}_y \otimes \tilde{B}_N - \tilde{D}_x^T H$, and the analogous properties of D_x, to obtain

$$
\begin{aligned}
A_1 &= \underbrace{(\mathbf{w}^m)^T (\tilde{H}_y \otimes \tilde{B}_N)\big(\mathbf{1}_x. \big(2\mu D_x \mathbf{v}^1 + \lambda(D_x \mathbf{v}^1 + D_y \mathbf{v}^2)\big)\big) + (\mathbf{w}^n)^T (\tilde{H}_y \otimes \tilde{B}_N)\big(\mathbf{1}_x. \big(\mu(D_y \mathbf{v}^1 + D_x \mathbf{v}^2)\big)\big)}_{\mathcal{B}_1} \\
&\quad - (\tilde{D}_x \mathbf{w}^m)^T H \mathbf{1}_x. \big(2\mu D_x \mathbf{v}^1 + \lambda(D_x \mathbf{v}^1 + D_y \mathbf{v}^2)\big) - (\tilde{D}_x \mathbf{w}^n)^T H \big(\mu(D_y \mathbf{v}^1 + D_x \mathbf{v}^2)\big) \\
&\quad + (\mathbf{w}^E)^T (H_y \otimes B_N)\big(\mathbf{1}_x. \big(\overset{b,x}{\mathbf{v}^1}. \big(2\mu D_x \mathbf{v}^1 + \lambda(D_x \mathbf{v}^1 + D_y \mathbf{v}^2)\big) + \mu \overset{b,x}{\mathbf{v}^2}.(D_y \mathbf{v}^1 + D_x \mathbf{v}^2)\big)\big) \\
&\quad - (D_x \mathbf{w}^E)^T H \mathbf{1}_x. \big(\overset{b,x}{\mathbf{v}^1}. \big(2\mu D_x \mathbf{v}^1 + \lambda(D_x \mathbf{v}^1 + D_y \mathbf{v}^2)\big) + \mu \overset{b,x}{\mathbf{v}^2}.(D_y \mathbf{v}^1 + D_x \mathbf{v}^2)\big).
\end{aligned}
$$

Consider the boundary terms, $\mathcal{B}_1$. Using the result (B.1) obtained in Appendix B, we find that

$$
\begin{aligned}
\mathcal{B}_1 &= \underbrace{(2\mu + \lambda)h_y (\mathbf{w}^m)^T \big(\mathbf{\underline{0}}, \quad \tilde{B}_N(\mathbf{1}_x. D_x \mathbf{v}^1)_{i,1}, \quad \tilde{B}_N(\mathbf{1}_x. D_x \mathbf{v}^1)_{i,2}, \quad \ldots \quad \tilde{B}_N(\mathbf{1}_x. D_x \mathbf{v}^1)_{i,M-1}, \quad \mathbf{\underline{0}}\big)^T}_{\mathcal{B}_{1,1}} \\
&\quad + \underbrace{\lambda h_y (\mathbf{w}^m)^T \big(\mathbf{\underline{0}}, \quad \tilde{B}_N(\mathbf{1}_x. D_y \mathbf{v}^2)_{i,1}, \quad \tilde{B}_N(\mathbf{1}_x. D_y \mathbf{v}^2)_{i,2}, \quad \ldots \quad \tilde{B}_N(\mathbf{1}_x. D_y \mathbf{v}^2)_{i,M-1}, \quad \mathbf{\underline{0}}\big)^T}_{\mathcal{B}_{1,2}} \\
&\quad + \underbrace{\mu h_y (\mathbf{w}^n)^T \big(\mathbf{\underline{0}}, \quad \tilde{B}_N(\mathbf{1}_x. D_y \mathbf{v}^1)_{i,1}, \quad \tilde{B}_N(\mathbf{1}_x. D_y \mathbf{v}^1)_{i,2}, \quad \ldots \quad \tilde{B}_N(\mathbf{1}_x. D_y \mathbf{v}^1)_{i,M-1}, \quad \mathbf{\underline{0}}\big)^T}_{\mathcal{B}_{1,3}} \\
&\quad + \underbrace{\mu h_y (\mathbf{w}^n)^T \big(\mathbf{\underline{0}}, \quad \tilde{B}_N(\mathbf{1}_x. D_x \mathbf{v}^2)_{i,1}, \quad \tilde{B}_N(\mathbf{1}_x. D_x \mathbf{v}^2)_{i,2}, \quad \ldots \quad \tilde{B}_N(\mathbf{1}_x. D_x \mathbf{v}^2)_{i,M-1}, \quad \mathbf{\underline{0}}\big)^T}_{\mathcal{B}_{1,4}}.
\end{aligned}
$$

Consider $\mathcal{B}_{1,1} + \mathcal{B}_{1,2}$. As they depend on the same component of the entropy variables, the terms can be rewritten as

$$
\mathcal{B}_{1,1} + \mathcal{B}_{1,2} = (2\mu + \lambda)h_y \sum_{j=1}^{M-1} (\mathbf{w}^m)_{i,j}^T (\tilde{B}_N(\mathbf{1}_x. D_x \mathbf{v}^1)_{i,j}) + \lambda h_y \sum_{j=1}^{M-1} (\mathbf{w}^m)_{i,j}^T (\tilde{B}_N(\mathbf{1}_x. D_y \mathbf{v}^2)_{i,j}).
$$

Consider an arbitrary node $j \neq \{0, M\}$, and neglect the parameters. Then we have

$$
\begin{aligned}
\mathcal{B}_{1,1} + \mathcal{B}_{1,2} &= \begin{pmatrix} w_{0,j}^m \\ w_{1,j}^m \\ \vdots \\ w_{N-1,j}^m \\ w_{N,j}^m \end{pmatrix}^T \begin{pmatrix} 0 & -\frac{1}{2} & 0 & 0 & 0 \ldots 0 \\ -\frac{1}{2} & 0 & 0 & 0 & 0 \ldots 0 \\ \vdots & & \ddots & & \vdots \\ 0 & \ldots & 0 & 0 & 0 & \frac{1}{2} \\ 0 & \ldots & 0 & 0 & \frac{1}{2} & 0 \end{pmatrix} \begin{pmatrix} (\mathbf{1}_x. D_x \mathbf{v}^1)_{0,j} \\ (\mathbf{1}_x. D_x \mathbf{v}^1)_{1,j} \\ \vdots \\ (\mathbf{1}_x. D_x \mathbf{v}^1)_{N-1,j} \\ (\mathbf{1}_x. D_x \mathbf{v}^1)_{N,j} \end{pmatrix} \\
&\quad + \begin{pmatrix} w_{0,j}^m \\ w_{1,j}^m \\ \vdots \\ w_{N-1,j}^m \\ w_{N,j}^m \end{pmatrix}^T \begin{pmatrix} 0 & -\frac{1}{2} & 0 & 0 & 0 \ldots 0 \\ -\frac{1}{2} & 0 & 0 & 0 & 0 \ldots 0 \\ \vdots & & \ddots & & \vdots \\ 0 & \ldots & 0 & 0 & 0 & \frac{1}{2} \\ 0 & \ldots & 0 & 0 & \frac{1}{2} & 0 \end{pmatrix} \begin{pmatrix} (\mathbf{1}_x. D_y \mathbf{v}^2)_{0,j} \\ (\mathbf{1}_x. D_y \mathbf{v}^2)_{1,j} \\ \vdots \\ (\mathbf{1}_x. D_y \mathbf{v}^2)_{N-1,j} \\ (\mathbf{1}_x. D_y \mathbf{v}^2)_{N,j} \end{pmatrix}, \\
&= \frac{1}{2}\big(-w_{1,j}^m (\mathbf{1}_x. D_x \mathbf{v}^1)_{0,j} - w_{0,j}^m (\mathbf{1}_x. D_x \mathbf{v}^1)_{1,j} + w_{N,j}^m (\mathbf{1}_x. D_x \mathbf{v}^1)_{N-1,j} + w_{N-1,j}^m (\mathbf{1}_x. D_x \mathbf{v}^1)_{N,j}\big) \\
&\quad + \frac{1}{2}\big(-w_{1,j}^m (\mathbf{1}_x. D_y \mathbf{v}^2)_{0,j} - w_{0,j}^m (\mathbf{1}_x. D_y \mathbf{v}^2)_{1,j} + w_{N,j}^m (\mathbf{1}_x. D_y \mathbf{v}^2)_{N-1,j} + w_{N-1,j}^m (\mathbf{1}_x. D_y \mathbf{v}^2)_{N,j}\big).
\end{aligned}
$$

Since $w_{0,j}^m = v_{0,j}^1 = 0$ and $w_{N,j}^m = v_{N,j}^1 = 0$, due to the no-slip condition, this reduces to

$$
\mathcal{B}_{1,1} + \mathcal{B}_{1,2} = \frac{1}{2}\big(-w_{1,j}^m (\mathbf{1}_x. D_x \mathbf{v}^1)_{0,j} + w_{N-1,j}^m (\mathbf{1}_x. D_x \mathbf{v}^1)_{N,j} - w_{1,j}^m (\mathbf{1}_x. D_y \mathbf{v}^2)_{0,j} + w_{N-1,j}^m (\mathbf{1}_x. D_y \mathbf{v}^2)_{N,j}\big).
$$

Next, we insert the specific form of the derivatives, which gives us

$$\mathcal{B}_{1,1} + \mathcal{B}_{1,2} = \frac{1}{2}\left(-w_{1,j}^m 1_{x_{0,j}} \frac{v_{1,j}^1 - v_{0,j}^1}{h_x} + w_{N-1,j}^m 1_{x_{N,j}} \frac{v_{N,j}^1 - v_{N-1,j}^1}{h_x}\right.$$
$$\left.- w_{1,j}^m 1_{x_{0,j}} \frac{v_{0,j+1}^1 - v_{0,j-1}^2}{2h_y} + w_{N-1,j}^m 1_{x_{N,j}} \frac{v_{N,j+1}^2 - v_{N,j-1}^2}{2h_y}\right).$$

Using the no-slip condition yet again, and inserting the specific expression of the entropy variable, we have

$$\mathcal{B}_{1,1} + \mathcal{B}_{1,2} = -\frac{1}{2h_x}\left(1_{x_{0,j}} \frac{(v_{1,j}^1)^2}{\mathrm{T}_{1,j}} + 1_{x_{N,j}} \frac{(v_{N-1,j}^1)^2}{\mathrm{T}_{N-1,j}}\right) \le 0, \qquad (\mathrm{T}_{i,j} > 0).$$

By analogous manipulations to $\mathcal{B}_{1,3} + \mathcal{B}_{1,4}$, A_1 reduces to

$$A_1 \le -(\tilde{D}_x \boldsymbol{w}^m)^T H \mathbf{1}_{\boldsymbol{x}}.\left(2\mu D_x \boldsymbol{v}^1 + \lambda(D_x \boldsymbol{v}^1 + D_y \boldsymbol{v}^2)\right) - (\tilde{D}_x \boldsymbol{w}^n)^T H \mathbf{1}_{\boldsymbol{x}}.\left(\mu(D_y \boldsymbol{v}^1 + D_x \boldsymbol{v}^2)\right)$$
$$+ \underbrace{(\boldsymbol{w}^E)^T (H_y \otimes B_N)\left(\mathbf{1}_{\boldsymbol{x}}.\left(\overset{b,x}{\boldsymbol{v}^1}.\left(2\mu D_x \boldsymbol{v}^1 + \lambda(D_x \boldsymbol{v}^1 + D_y \boldsymbol{v}^2)\right) + \mu \overset{b,x}{\boldsymbol{v}^2}.(D_y \boldsymbol{v}^1 + D_x \boldsymbol{v}^2)\right)\right)}_{\mathcal{B}_2}$$
$$- (D_x \boldsymbol{w}^E)^T H \mathbf{1}_{\boldsymbol{x}}.\left(\overset{b,x}{\boldsymbol{v}^1}.\left(2\mu D_x \boldsymbol{v}^1 + \lambda(D_x \boldsymbol{v}^1 + D_y \boldsymbol{v}^2)\right) + \mu \overset{b,x}{\boldsymbol{v}^2}.(D_y \boldsymbol{v}^1 + D_x \boldsymbol{v}^2)\right).$$

The boundary term, $\mathcal{B}_2$, is produced by the (2,1)-SBP operator, and from the SBP-properties in Section 3, we know it will extract boundary terms (in contrast to the $\tilde{B}$s, which extract terms along the boundaries *and* the neighbouring nodes). Since $\overset{b,x}{\boldsymbol{v}^1} = \overset{b,x}{\boldsymbol{v}^2} = 0$ at the boundaries (see (37)), it follows that all boundary terms vanish. The resulting estimate is therefore

$$A_1 \le -(\tilde{D}_x \boldsymbol{w}^m)^T H \mathbf{1}_{\boldsymbol{x}}.\left(2\mu D_x \boldsymbol{v}^1 + \lambda(D_x \boldsymbol{v}^1 + D_y \boldsymbol{v}^2)\right) - (\tilde{D}_x \boldsymbol{w}^n)^T H \mathbf{1}_{\boldsymbol{x}}.\left(\mu(D_y \boldsymbol{v}^1 + D_x \boldsymbol{v}^2)\right)$$
$$- (D_x \boldsymbol{w}^E)^T H \mathbf{1}_{\boldsymbol{x}}.\left(\overset{b,x}{\boldsymbol{v}^1}.\left(2\mu D_x \boldsymbol{v}^1 + \lambda(D_x \boldsymbol{v}^1 + D_y \boldsymbol{v}^2)\right) + \mu \overset{b,x}{\boldsymbol{v}^2}.(D_y \boldsymbol{v}^1 + D_x \boldsymbol{v}^2)\right). \tag{73}$$

Similarly for the viscous flux in the y-direction, we multiply (66) by the entropy variables and the norm matrix, H, to end up with

$$A_2 \le -(\tilde{D}_y \boldsymbol{w}^m)^T H \mathbf{1}_{\boldsymbol{y}}.(\mu(D_y \boldsymbol{v}^1 + D_x \boldsymbol{v}^2)) - (\tilde{D}_y \boldsymbol{w}^n)^T H \mathbf{1}_{\boldsymbol{y}}.(2\mu D_y \boldsymbol{v}^2) + \lambda(D_x \boldsymbol{v}^1 + D_y \boldsymbol{v}^2)$$
$$- (D_y \boldsymbol{w}^E)^T H \mathbf{1}_{\boldsymbol{y}}.\left(\overset{b,y}{\boldsymbol{v}^2}.(2\mu D_y \boldsymbol{v}^2 + \lambda(D_x \boldsymbol{v}^1 + D_y \boldsymbol{v}^2)) + \mu \overset{b,y}{\boldsymbol{v}^1}.(D_y \boldsymbol{v}^1 + D_x \boldsymbol{v}^2)\right) \tag{74}$$

Combining (73) and (74), we obtain

$$\boldsymbol{w}^T \mathbf{H} \mathcal{D}_x^v \boldsymbol{f}^\mu + \boldsymbol{w}^T \mathbf{H} \mathcal{D}_y^v \boldsymbol{g}^\mu \le -(\tilde{D}_x \boldsymbol{w}^m)^T H \mathbf{1}_{\boldsymbol{x}}.\left(2\mu D_x \boldsymbol{v}^1 + \lambda(D_x \boldsymbol{v}^1 + D_y \boldsymbol{v}^2)\right) - (\tilde{D}_x \boldsymbol{w}^n)^T H \mathbf{1}_{\boldsymbol{x}}.\left(\mu(D_y \boldsymbol{v}^1 + D_x \boldsymbol{v}^2)\right)$$
$$- (D_x \boldsymbol{w}^E)^T H \mathbf{1}_{\boldsymbol{x}}.\left(\overset{b,x}{\boldsymbol{v}^1}.\left(2\mu D_x \boldsymbol{v}^1 + \lambda(D_x \boldsymbol{v}^1 + D_y \boldsymbol{v}^2)\right) + \mu \overset{b,x}{\boldsymbol{v}^2}.(D_y \boldsymbol{v}^1 + D_x \boldsymbol{v}^2)\right)$$
$$- (\tilde{D}_y \boldsymbol{w}^m)^T H \mathbf{1}_{\boldsymbol{y}}.(\mu(D_y \boldsymbol{v}^1 + D_x \boldsymbol{v}^2)) - (\tilde{D}_y w^n)^T H \mathbf{1}_{\boldsymbol{y}}.(2\mu D_y \boldsymbol{v}^2) + \lambda(D_x \boldsymbol{v}^1 + D_y \boldsymbol{v}^2)$$
$$- (D_y \boldsymbol{w}^E)^T H \mathbf{1}_{\boldsymbol{y}}.\left(\overset{b,y}{\boldsymbol{v}^2}.(2\mu D_y \boldsymbol{v}^2 + \lambda(D_x \boldsymbol{v}^1 + D_y \boldsymbol{v}^2)) + \mu \overset{b,y}{\boldsymbol{v}^1}.(D_y \boldsymbol{v}^1 + D_x \boldsymbol{v}^2)\right). \tag{75}$$

To recast (75) as a quadratic form, we use the entropy variables (71) and utilise that the derivative operators satisfy the discrete product rule (39). Then,

$$\boldsymbol{w}^T \mathbf{H}(\mathcal{D}_x^v \boldsymbol{f}^\mu + \mathcal{D}_y^v \boldsymbol{g}^\mu) \le -\frac{1}{c_v}\left(\left(\overset{b,x}{\boldsymbol{v}^1}.\tilde{D}_x \mathrm{T}^{-1} + \overset{i,x}{\mathrm{T}^{-1}}.\tilde{D}_x \boldsymbol{v}^1\right)^T H \mathbf{1}_{\boldsymbol{x}}.\left(2\mu D_x \boldsymbol{v}^1 + \lambda(D_x \boldsymbol{v}^1 + D_y \boldsymbol{v}^2)\right)\right)$$
$$- \frac{1}{c_v}\left(\left(\overset{b,x}{\boldsymbol{v}^2}.\tilde{D}_x \mathrm{T}^{-1} + \overset{i,x}{\mathrm{T}^{-1}}.\tilde{D}_x \boldsymbol{v}^2\right)^T H \mathbf{1}_{\boldsymbol{x}}.\left(\mu(D_y \boldsymbol{v}^1 + D_x \boldsymbol{v}^2)\right)\right)$$
$$+ \frac{1}{c_v}\left((D_x \mathrm{T}^{-1})^T H \mathbf{1}_{\boldsymbol{x}}.\left(\overset{b,x}{\boldsymbol{v}^1}.\left(2\mu D_x \boldsymbol{v}^1 + \lambda(D_x \boldsymbol{v}^1 + D_y \boldsymbol{v}^2)\right) + \mu \overset{b,x}{\boldsymbol{v}^2}.(D_y \boldsymbol{v}^1 + D_x \boldsymbol{v}^2)\right)\right)$$
$$- \frac{1}{c_v}\left(\left(\overset{b,y}{\boldsymbol{v}^1}.\tilde{D}_y \mathrm{T}^{-1} + \overset{i,y}{\mathrm{T}^{-1}}.\tilde{D}_y \boldsymbol{v}^1\right)^T H \mathbf{1}_{\boldsymbol{y}}.\left(\mu(D_y \boldsymbol{v}^1 + D_x \boldsymbol{v}^2)\right)\right)$$

$$-\frac{1}{c_v}\left(\left(\overset{b,y}{\underline{\boldsymbol{v}^2.\tilde{D}_y\mathrm{T}^{-1}}}+\overset{i,y}{\mathrm{T}^{-1}.\tilde{D}_y\boldsymbol{v}^2}\right)^T H\mathbf{1}_{\boldsymbol{y}}.(2\mu D_y\boldsymbol{v}^2+\lambda(D_x\boldsymbol{v}^1+D_y\boldsymbol{v}^2))\right)$$

$$+\frac{1}{c_v}\left((D_y\mathrm{T}^{-1})^T H\mathbf{1}_{\boldsymbol{y}}.\left(\overset{b,y}{\underline{\boldsymbol{v}^2}}.(2\mu D_y\boldsymbol{v}^2+\lambda(D_x\boldsymbol{v}^1+D_y\boldsymbol{v}^2))+\overset{b,y}{\underline{\mu\boldsymbol{v}^1}}.(D_y\boldsymbol{v}^1+D_x\boldsymbol{v}^2)\right)\right).$$

A number of terms cancel (see the colour code above), and we end up with

$$\boldsymbol{w}^T\mathbf{H}(\mathcal{D}_x^{\mathsf{v}}\mathbf{f}^\mu+\mathcal{D}_y^{\mathsf{v}}\mathbf{g}^\mu)\leq-\frac{1}{c_v}\left((\overset{i,x}{\mathrm{T}^{-1}.\tilde{D}_x\boldsymbol{v}^1})^T H\mathbf{1}_{\boldsymbol{x}}.(2\mu D_x\boldsymbol{v}^1+\lambda(D_x\boldsymbol{v}^1+D_y\boldsymbol{v}^2))+(\overset{i,x}{\mathrm{T}^{-1}.\tilde{D}_x\boldsymbol{v}^2})^T H\mathbf{1}_{\boldsymbol{x}}.(\mu(D_y\boldsymbol{v}^1+D_x\boldsymbol{v}^2))\right)$$

$$-\frac{1}{c_v}\left((\overset{i,y}{\mathrm{T}^{-1}.\tilde{D}_y\boldsymbol{v}^1})^T H\mathbf{1}_{\boldsymbol{y}}.(\mu(D_y\boldsymbol{v}^1+D_x\boldsymbol{v}^1))+(\overset{i,y}{\mathrm{T}^{-1}.\tilde{D}_y\boldsymbol{v}^2})^T H\mathbf{1}_{\boldsymbol{y}}.(2\mu D_y\boldsymbol{v}^2+\lambda(D_x\boldsymbol{v}^1+D_y\boldsymbol{v}^2))\right).$$

Use the form of $\mathbf{1}_{\boldsymbol{x}}$ and $\mathbf{1}_{\boldsymbol{y}}$ from (67) and Stokes' hypothesis, $\lambda=-\frac{2}{3}\mu$, to obtain

$$\boldsymbol{w}^T\mathbf{H}(\mathcal{D}_x^{\mathsf{v}}\mathbf{f}^\mu+\mathcal{D}_y^{\mathsf{v}}\mathbf{g}^\mu)\leq-\frac{\mu}{c_v}\left(\frac{4}{3}(\tilde{D}_x\boldsymbol{v}^1)^T H(\mathrm{T}^{-1}.D_x\boldsymbol{v}^1)-\frac{2}{3}(\tilde{D}_x\boldsymbol{v}^1)^T H(\mathrm{T}^{-1}.D_y\boldsymbol{v}^2)\right.$$

$$+(\tilde{D}_x\boldsymbol{v}^2)^T H(\mathrm{T}^{-1}.D_y\boldsymbol{v}^1)+(\tilde{D}_x\boldsymbol{v}^2)^T H(\mathrm{T}^{-1}.D_x\boldsymbol{v}^2)$$

$$+(\tilde{D}_y\boldsymbol{v}^1)^T H(\mathrm{T}^{-1}.D_y\boldsymbol{v}^1)+(\mathrm{T}^{-1}.\tilde{D}_y\boldsymbol{v}^1)^T H(D_x\boldsymbol{v}^2)$$

$$\left.-\frac{2}{3}(\tilde{D}_y\boldsymbol{v}^2)^T H(\mathrm{T}^{-1}.D_x\boldsymbol{v}^1)+\frac{4}{3}(\tilde{D}_y\boldsymbol{v}^2)^T H(\mathrm{T}^{-1}.D_y\boldsymbol{v}^2)\right),$$

which can be further rearranged into

$$\boldsymbol{w}^T\mathbf{H}(\mathcal{D}_x^{\mathsf{v}}\mathbf{f}^\mu+\mathcal{D}_y^{\mathsf{v}}\mathbf{g}^\mu)\leq-\frac{\mu}{c_v}\left(\frac{2}{3}\begin{pmatrix}(\tilde{D}_x\boldsymbol{v}^1)^T\\(\tilde{D}_y\boldsymbol{v}^2)^T\end{pmatrix}^T\begin{pmatrix}H&-H\\-H&H\end{pmatrix}\begin{pmatrix}\mathrm{T}^{-1}.D_x\boldsymbol{v}^1\\\mathrm{T}^{-1}.D_y\boldsymbol{v}^2\end{pmatrix}+\begin{pmatrix}(\tilde{D}_x\boldsymbol{v}^2)^T\\(\tilde{D}_y\boldsymbol{v}^1)^T\end{pmatrix}^T\begin{pmatrix}H&H\\H&H\end{pmatrix}\begin{pmatrix}\mathrm{T}^{-1}.D_x\boldsymbol{v}^2\\\mathrm{T}^{-1}.D_y\boldsymbol{v}^1\end{pmatrix}\right.$$

$$\left.+\frac{2}{3}\|\sqrt{\mathrm{T}^{-1}}.\tilde{D}_x\boldsymbol{v}^1\|_H^2+\frac{2}{3}\|\sqrt{\mathrm{T}^{-1}}.\tilde{D}_y\boldsymbol{v}^2\|_H^2\right)\leq 0,\qquad(\mathrm{T}>0)$$

i.e., (72) holds true. $\square$

Lemma 5.6. *The diffusive heat fluxes* (68) *satisfy*

$$\boldsymbol{w}^T\mathbf{H}\mathcal{D}_x^{\mathsf{v}}\mathbf{f}^\kappa+\boldsymbol{w}^T\mathbf{H}\mathcal{D}_y^{\mathsf{v}}\mathbf{g}^\kappa+\boldsymbol{w}^T\mathbf{HSAT}\leq 0.\tag{76}$$

Proof. Denote the left-hand side of (76) by A, then

$$A=\kappa\left((\boldsymbol{w}^E)^T HD_xD_x\mathrm{T}+(\boldsymbol{w}^E)^T HD_yD_y\mathrm{T}\right)+(\boldsymbol{w}^E)^T\mathbf{HSAT},$$

$$=\kappa\left((\boldsymbol{w}^E)^T(H_y\otimes H_x)(I_y\otimes D_N)D_x\mathrm{T}+(\boldsymbol{w}^E)^T(H_x\otimes H_y)(D_M\otimes I_x)D_y\mathrm{T}\right)+(\boldsymbol{w}^E)^T\mathbf{HSAT}.$$

This can be stated more compactly as

$$A=\kappa\left((\boldsymbol{w}^E)^T(H_y\otimes Q_N)D_x\mathrm{T}+(\boldsymbol{w}^E)^T(Q_M\otimes H_x)D_y\mathrm{T}\right)+(\boldsymbol{w}^E)^T\mathbf{HSAT}.$$

Utilising that $Q=B-Q^T$, we obtain

$$A=\kappa\left(\underbrace{-(\boldsymbol{w}^E)^T(H_y\otimes Q_N^T)D_x\mathrm{T}-(\boldsymbol{w}^E)^T(Q_M^T\otimes H_x)D_y\mathrm{T}}_{A_1}\right.$$

$$\left.\underbrace{+(\boldsymbol{w}^E)^T(H_y\otimes B_N)D_x\mathrm{T}+(\boldsymbol{w}^E)^T(B_M\otimes H_x)D_y\mathrm{T}}_{A_2}\right)+(\boldsymbol{w}^E)^T\mathbf{HSAT}.$$

Manipulations of A_1 give us

$$A_1 = -\kappa \left((\boldsymbol{w}^E)^T (I_y \otimes D_N)^T (H_y \otimes H_x) D_x \mathrm{T} + (\boldsymbol{w}^E)^T (D_M \otimes I_x)^T (H_y \otimes H_x) D_y \mathrm{T} \right),$$

$$= -\kappa \left((D_x \boldsymbol{w}^E)^T H D_x \mathrm{T} + (D_y \boldsymbol{w}^E)^T H D_y \mathrm{T} \right).$$

Recall that $\boldsymbol{w}^E = -\frac{1}{c_v \mathrm{T}}$, such that, by using the discrete quotient rule (40), the above is equivalent to

$$A_1 = -\frac{\kappa}{c_v} \left(((\mathrm{T}^2)^{-1} . D_x \mathrm{T})^T H D_x \mathrm{T} + ((\mathrm{T}^2)^{-1} . D_y \mathrm{T})^T H D_y \mathrm{T} \right) = -\frac{\kappa}{c_v} \left(\| \sqrt{(\overset{x}{\mathrm{T}^2})^{-1}} . D_x \mathrm{T} \|_H^2 + \| \sqrt{(\overset{y}{\mathrm{T}^2})^{-1}} . D_y \mathrm{T} \|_H^2 \right),$$

where $(\overset{x}{\mathrm{T}^2})^{-1}$ and $(\overset{y}{\mathrm{T}^2})^{-1}$ are vectors containing the coefficients produced by the quotient rule (40).

Next, consider the boundary terms A_2, and insert the specific form of the SAT:

$$A_2 = \kappa \left((\boldsymbol{w}^E)^T (H_y \otimes B_N) D_x \mathrm{T} + (\boldsymbol{w}^E)^T (B_M \otimes H_x) D_y \mathrm{T} \right)$$

$$- \kappa (\boldsymbol{w}^E)^T (H_y \otimes H_x) \left((I_M \otimes H_x^{-1} B_N)(D_x \mathrm{T}) + (H_y^{-1} B_M \otimes I_N)(D_y \mathrm{T}) \right),$$

$$= \kappa (\boldsymbol{w}^E)^T \left((H_y \otimes B_N) D_x \mathrm{T} + (B_M \otimes H_x) D_y \mathrm{T} - (H_y \otimes B_N) D_x \mathrm{T} - (B_M \otimes H_x) D_y \mathrm{T} \right) = 0.$$

Hence, we have

$$\boldsymbol{w}^T H \mathcal{D}_x^\vee \boldsymbol{f}^\kappa + \boldsymbol{w}^T H \mathcal{D}_y^\vee \boldsymbol{g}^\kappa + \boldsymbol{w}^T H \mathsf{SAT} = -\frac{\kappa}{c_v} \left(\| \sqrt{(\overset{x}{\mathrm{T}^2})^{-1}} . D_x \mathrm{T} \|_H^2 + \| \sqrt{(\overset{y}{\mathrm{T}^2})^{-1}} . D_y \mathrm{T} \|_H^2 \right) \leq 0. \quad \square$$

Proposition 5.7. *The semi-discrete scheme* (69) *is entropy stable in the sense of* (52).

Proof. Contract (69) with $\boldsymbol{w}_{i,j}^T = -\frac{1}{c_v \mathrm{T}_{i,j}} \left(\frac{(v_{i,j}^1)^2 + (v_{i,j}^2)^2}{2} + c_v \mathrm{T}_{i,j} (\mathcal{S}_{i,j} - \gamma), -v_{i,j}^1, -v_{i,j}^2, 1 \right)$, and the corresponding diagonal norm matrix element, H_k, $(k = (j(N+1) + i))$. Then sum over all grid points:

$$\sum_{i,j=0}^{N,M} \boldsymbol{w}_{i,j}^T H_k (\boldsymbol{u}_{i,j})_t + \boldsymbol{w}_{i,j}^T H_k (\mathcal{D}_x^\mathsf{I} \boldsymbol{f})_{i,j} + \boldsymbol{w}_{i,j}^T H_k (\mathcal{D}_y^\mathsf{I} \boldsymbol{g})_{i,j},$$

$$= \sum_{i,j=0}^{N,M} \left(\boldsymbol{w}_{i,j}^T H_k (\mathcal{D}_x^\vee \boldsymbol{f}^\mu)_{i,j} + \boldsymbol{w}_{i,j}^T H_k (\mathcal{D}_x^\vee \boldsymbol{f}^\kappa)_{i,j} + \boldsymbol{w}_{i,j}^T H_k (\mathcal{D}_y^\vee \boldsymbol{g}^\mu)_{i,j} + \boldsymbol{w}_{i,j}^T H_k (\mathcal{D}_y^\vee \boldsymbol{g}^\kappa)_{i,j} + \boldsymbol{w}_{i,j}^T H_k \mathsf{SAT}_{i,j} \right).$$

By Lemma 5.4 the inviscid flux approximations on the left-hand side have been demonstrated to be entropy stable, hence we have

$$\sum_{i,j=0}^{N,M} H_k (U_{i,j})_t \leq \sum_{i,j=0}^{N,M} \left(\boldsymbol{w}_{i,j}^T H_k (\mathcal{D}_x^\vee \boldsymbol{f}^\mu)_{i,j} + \boldsymbol{w}_{i,j}^T H_k (\mathcal{D}_x^\vee \boldsymbol{f}^\kappa)_{i,j} + \boldsymbol{w}_{i,j}^T H_k (\mathcal{D}_y^\vee \boldsymbol{g}^\mu)_{i,j} + \boldsymbol{w}_{i,j}^T H_k (\mathcal{D}_y^\vee \boldsymbol{g}^\kappa)_{i,j} + \boldsymbol{w}_{i,j}^T H_k \mathsf{SAT}_{i,j} \right).$$

Note that the sum on the right-hand side is equivalent to the matrix multiplications:

$$\sum_{i,j=0}^{N,M} \left(\boldsymbol{w}_{i,j}^T H_k (\mathcal{D}_x^\vee \boldsymbol{f}^\mu)_{i,j} + \boldsymbol{w}_{i,j}^T H_k (\mathcal{D}_x^\vee \boldsymbol{f}^\kappa)_{i,j} + \boldsymbol{w}_{i,j}^T H_k (\mathcal{D}_y^\vee \boldsymbol{g}^\mu)_{i,j} + \boldsymbol{w}_{i,j}^T H_k (\mathcal{D}_y^\vee \boldsymbol{g}^\kappa)_{i,j} + \boldsymbol{w}_{i,j}^T H_k \mathsf{SAT}_{i,j} \right),$$

$$= \boldsymbol{w}^T H \mathcal{D}_x^\vee \boldsymbol{f}^\mu + \boldsymbol{w}^T H \mathcal{D}_y^\vee \boldsymbol{g}^\mu + \boldsymbol{w}^T H \mathcal{D}_x^\vee \boldsymbol{f}^\kappa + \boldsymbol{w}^T H \mathcal{D}_y^\vee \boldsymbol{g}^\kappa + \boldsymbol{w}^T H \mathsf{SAT},$$

such that we can utilise the results of Lemma 5.5 and 5.6, and obtain

$$\sum_{i,j=0}^{N,M} H_k (U_{i,j})_t \leq 0. \quad \square$$

6. Numerical simulations

To demonstrate the properties of the schemes with special emphasis on the no-slip condition, we consider both a subsonic and a supersonic case.
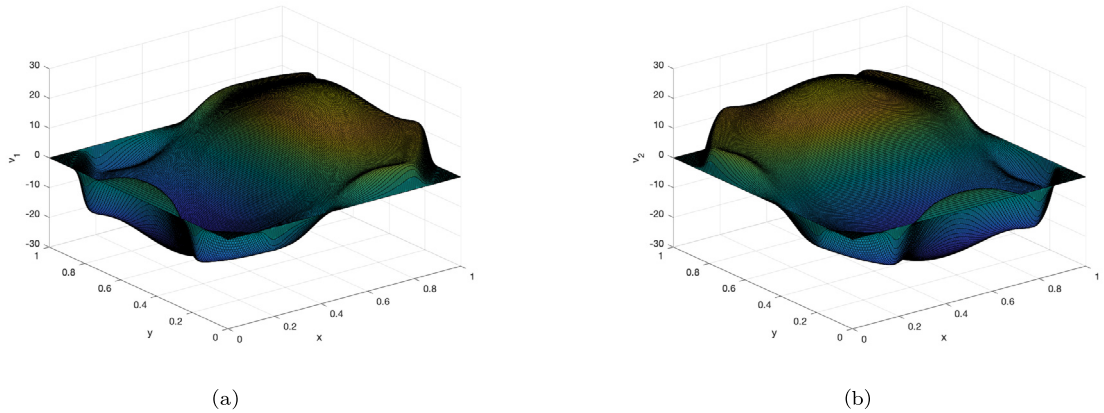
(a)

(b)

Fig. 1. (a) v_1 at $t = 0.01$ obtained with 257^2 grid points and $\alpha = 1$. (b) v_2 at $t = 0.01$ obtained with 257^2 grid points and $\alpha = 1$.
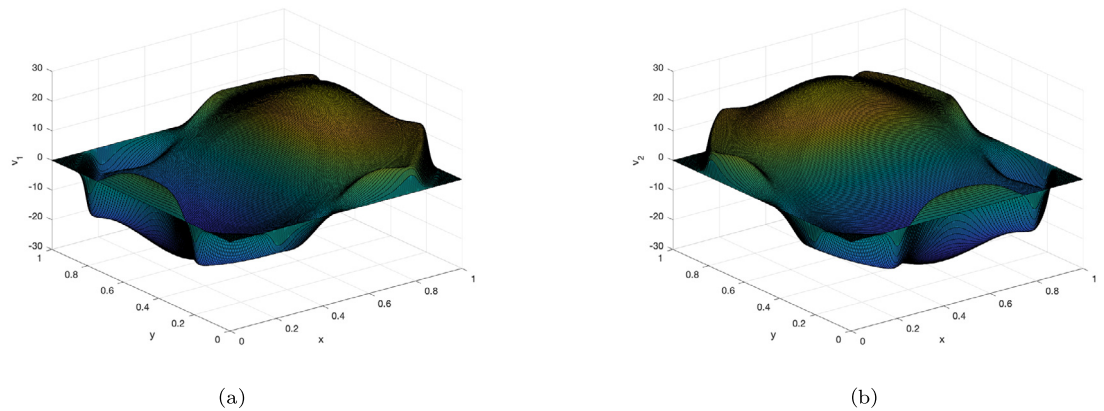

(a)

(b)

Fig. 2. (a) v_1 at $t = 0.01$ obtained with 257^2 grid points and $\alpha = 0.4$. (b) v_2 at $t = 0.01$ obtained with 257^2 grid points and $\alpha = 0.4$.

6.1. Blast wave

Let $\Omega = [0, 1] \times [0, 1]$, with homogeneous no-slip condition at all walls. We use a similar setup as in [26] with the following initial conditions

$$\rho = 1, \qquad v_1 = 0, v_2 = 0, \qquad p = \begin{cases} 0.01, & \text{if } (x, y) \in \Omega \setminus \mathcal{B}((0.5, 0.5), 0.35), \\ 1000, & \text{if } (x, y) \in \mathcal{B}((0.5, 0.5), 0.35), \end{cases}$$

where $\mathcal{B}((0.5, 0.5), 0.35)$ denotes a disk centred at $(x, y) = (0.5, 0.5)$ with radius $r = 0.35$. Furthermore, we use the following parameters

$$\gamma = 1.4, \qquad \mathcal{R} = 286.84, \qquad \mu = 0.1, \qquad \text{Pr} = 0.72, \qquad c_p = 1005, \qquad \kappa = \frac{\mu c_p}{\text{Pr}}.$$

We use (69) with, $\delta_{i+1/2, j} = \alpha \max \left(\left| v^1_{i,j} \right| + c_{i,j}, \left| v^1_{i+1,j} \right| + c_{i+1,j} \right)$. For $\alpha = 1$, this is the entropy stable local Lax-Friedrichs scheme, but to stress test the scheme we also run the non-provably entropy stable choice $\alpha = 0.4$. For time discretisation, we apply the third-order strong stability preserving Runge-Kutta method (see [7]).

The entropy-stable numerical results computed with 257^2 grid points and $\alpha = 1$ are displayed in Fig. 1a and 1b at time $t = 0.01$. Fig. 2a and 2b display the numerical results obtained for the same problem, but with reduced artificial diffusion, $\alpha = 0.4$.

Lastly, we have run a simulation on a coarse mesh (33^2 grid points) as a further demonstration of the robustness of the boundary treatment. The results for the velocity components are displayed in Fig. 3a and 3b.

We have furthermore compared the entropy decay for the cases $\alpha = 1$ and $\alpha = 0.4$ (for the coarse mesh to highlight the differences). The plot of the total entropy, i.e., $\int_\Omega U(u) \, d\Omega$ is depicted in Fig. 4. We have normalised the entropy at every time step by subtracting the initial entropy, $\int_\Omega U(u) \, d\Omega \big|_{t=0}$. As we see from the plot, the entropy is decaying for both values of α, but the decay is faster for larger diffusion, which is as expected.

(a)   (b)
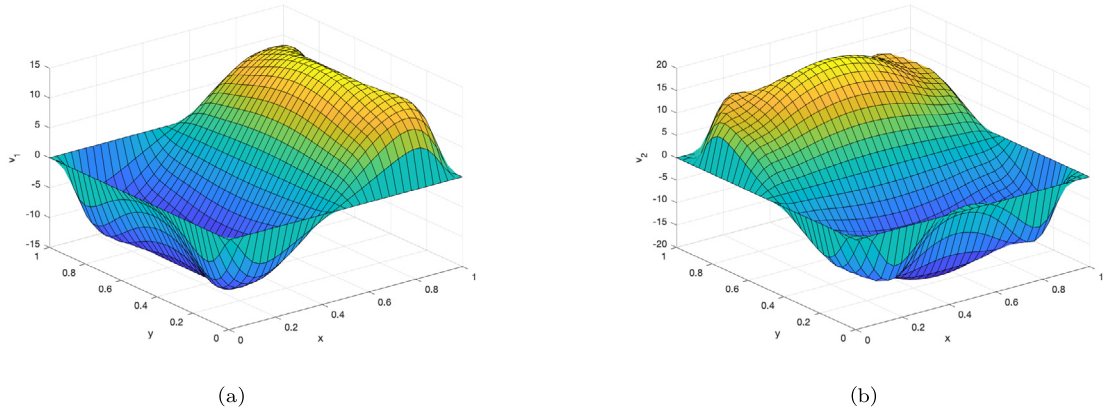
Fig. 3. (a) v_1 at $t = 0.01$ obtained with 33^2 grid points and $\alpha = 1$. (b) v_2 at $t = 0.01$ obtained with 33^2 grid points and $\alpha = 0.4$.
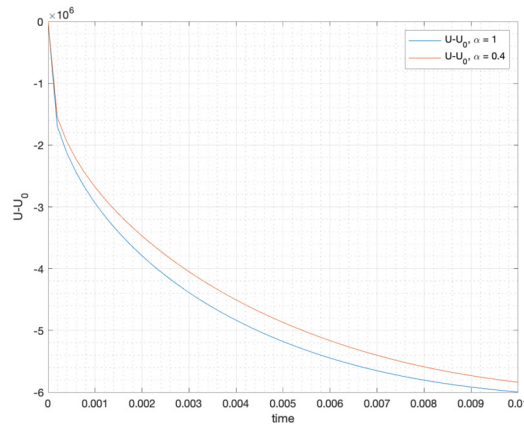
Fig. 4. Plot of the (normalised) total entropy $\int_\Omega U(u)\, d\Omega\big|_{t=t} - \int_\Omega U(u)\, d\Omega\big|_{t=0}$ for the coarse grid with $\alpha = 1$ and $\alpha = 0.4$.

6.2. Lid-driven cavity flow

We have run a similar problem as in [3] on the spatial domain $\Omega = [0, 1] \times [0, 1]$. The upper wall of the cavity is moving at a constant speed to the right, such that the boundary conditions for the velocity components become

$$\begin{cases} v_1 = 1, v_2 = 0, & \partial\Omega \cap \{y = 1\}, \\ v_{1,2} = 0, & \partial\Omega \setminus \{y = 1\}. \end{cases} \tag{77}$$

The boundary condition for the temperature is given by (62). Furthermore, the problem parameters are given by $Re = 100$, $Ma = 0.1$, $\text{Pr} = 0.72$, $\gamma = 1.4$, and it is initialised by the conditions

$$\rho = 1, \qquad v_1, v_2 = 0, \qquad p = \frac{1}{Ma^2\gamma}.$$

Note that at one wall, the lid-driven cavity problem has a non-homogeneous no-slip condition for one of the velocity components. Still, an entropy bound for the continuum solution is obtained as only the normal components of the velocities enter the estimate. (We have not been able to prove entropy stability for the discrete scheme with the boundary conditions (77).)

Fig. 5a shows the solution at $t = 2$ when using the scheme (69). We have also run the same problem using a 3rd-order scheme. (See remark at the end of Section 5.1.) We have verified linear stability in one spatial dimension, and the extension to two dimensions is straightforward. The 3rd-order numerical solution is shown in Fig. 5b.

Fig. 6a shows the solution at $t = 2$ for the lid-driven cavity flow with the heat-entropy flow boundary condition $\frac{\kappa}{T}\frac{\partial T}{\partial n} = g = 2$. The solution is qualitatively similar to the adiabatic case where $\frac{\partial T}{\partial n} = 0$. Fig. 6b depicts the total entropy $\int_\Omega U(u)\, d\Omega$, normalised by subtracting the initial entropy $\int_\Omega U(u)|_0\, d\Omega$. We note that the entropy increases initially. This does not violate the entropy inequality since the system is not closed; there is a heat-entropy flow through the boundary.
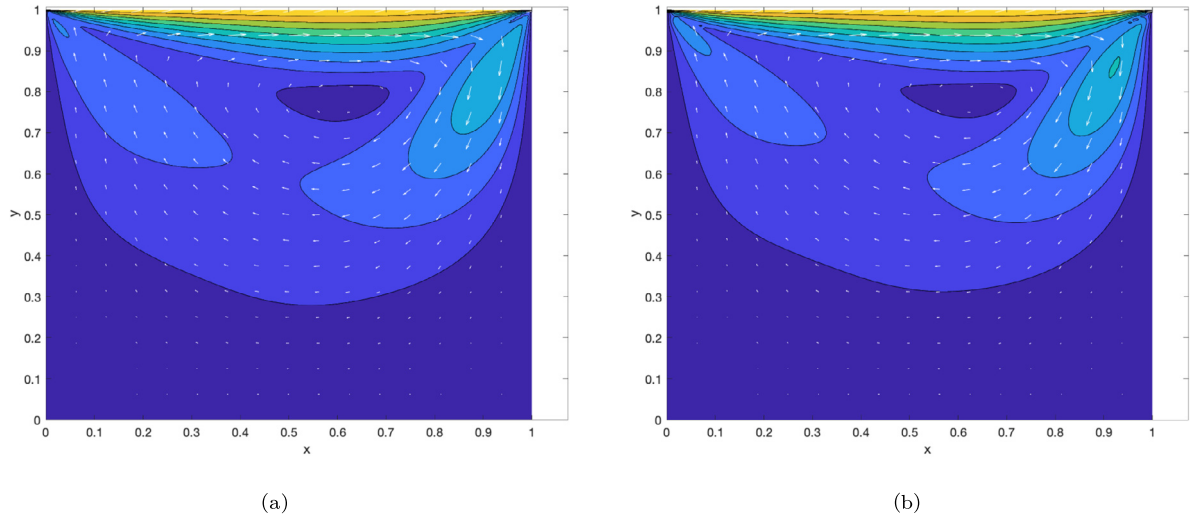
(a)

(b)

Fig. 5. (a) The velocity field displayed at $t = 2$ using 257^2 grid points and $\alpha = 0.15$. (Second-order scheme.) (b) The velocity field displayed at $t = 2$ using 129^2 grid points. (3rd-order SBP scheme.)
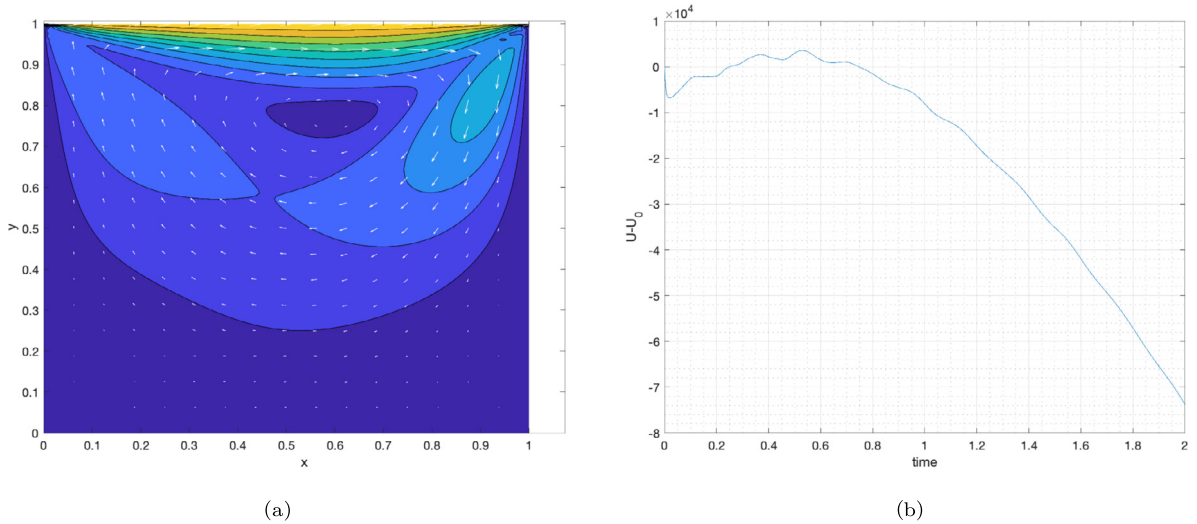

(a)

(b)

Fig. 6. (a) The velocity field displayed at $t = 2$ using 129^2 grid points. (Second-order scheme using the heat entropy flow boundary condition.) (b) The velocity field displayed at $t = 2$ using 129^2 grid points. (Second-order scheme using the heat entropy flow boundary condition.)

6.2.1. Comments for the implementation

Since one of the velocity components is non-zero at the boundary $y = 1$ for the lid-driven cavity, we must manually update this boundary after each Runge-Kutta stage even when using the proposed scheme with the Dirichlet-SBP operator. This is to take into account the contribution from the continuity equation into the momentum equation at the boundary. The momentum equation is updated as $m|_{\partial\Omega,\{y=1\}} = \rho|_{\partial\Omega,\{y=1\}} v_1|_{\partial\Omega,\{y=1\}}$, where $\rho|_{\partial\Omega,\{y=1\}}$ is given by the continuity equation and $v_1|_{\partial\Omega,\{y=1\}} = 1$.

7. Conclusions

In this article, we have investigated the injection method for strongly imposing the no-slip condition for finite-difference approximations of the compressible Navier-Stokes equations in 1-D and 2-D. Based on standard SBP operators, spatial operators (which we have termed Dirichlet-SBP operators) facilitating the injection procedure were introduced. The temperature condition, on the other hand, was enforced by a SAT. Thus, density, pressure and temperature are updated on the boundary while the momentum is no longer a variable in the boundary points. In particular, we have considered the stability properties of the proposed schemes taking the mixed boundary treatment into account.

When proving linear stability of non-linear problems, it is common to immediately associate the scheme with a linear symmetric constant-coefficient version. Herein, we have rigorously performed all linearisation steps for two different

schemes; one with second-order interior accuracy and one with fourth-order. We prove that the procedure is valid for the proposed 1-D scheme, including the strong-weak imposition of the wall boundary conditions. The linearisation of the 2-D scheme requires considerable more work, but we do not see any additional difficulties beyond more involved algebra and it should also reduce to the same form as the 1-D scheme. Moreover, under the assumption that the interior scheme is entropy stable (52), we have proven that both the proposed 1-D and 2-D 2nd-order schemes, with the mixed boundary treatment, are non-linearly (entropy) stable. The non-linear stability proofs are straightforwardly extendable to 3-D.

Although our proofs rely on the introduction of the Dirichlet-SBP operator, we stress that this operator is not necessary in practice, and has only been introduced for purpose of the proofs. In implementations one can simply overwrite the velocity at the boundary nodes after each Runge-Kutta stage. (This makes the code significantly simpler than with SATs enforcing no-slip.)

Two numerical test cases have been considered; a blast wave and a lid-driven cavity flow. For the blast wave, two types of local Lax-Friedrichs type diffusions were considered: an entropy stable diffusion ($\alpha = 1$) and a non-provably entropy stable diffusion ($\alpha = 0.4$). In both cases, the total entropy was decaying, although a faster decay was observed for the more diffusive scheme (which is as expected). For the lid-driven cavity flow, a reduced local Lax-Friedrichs diffusion ($\alpha = 0.15$) was considered for the 2nd-order scheme. Thereafter, the 3rd-order, linearly stable (but not provably non-linearly stable), scheme was run. The solutions were similar to those obtained in [3]. All test cases demonstrated that the combination of strongly and weakly imposed boundary conditions is robust, and corroborate the claim that the 2-D scheme is stable.

CRediT authorship contribution statement

Anita Gjesteland: Conceptualization, Formal analysis, Software, Writing – original draft, Writing – review & editing. **Magnus Svärd:** Conceptualization, Formal analysis, Methodology, Writing – review & editing.

Declaration of competing interest

The authors declare that they have no known competing financial interests or personal relationships that could have appeared to influence the work reported in this paper.

Data availability

Data will be made available on request.

Appendix A. Linearisation procedure

A.1. Linearisation of the compressible Navier-Stokes equations in 1D

We present the derivation of the linearised and symmetrised Navier-Stokes equations (13), since the details are not presented in [1].

We write the Navier-Stokes equations (10) in primitive variables $v = (\rho, v, p)^T$:

$$\rho_t + (\rho v)_x = 0, \tag{A.1}$$

$$v_t + v v_x + \frac{1}{\rho} p_x = \frac{2\mu + \lambda}{\rho} v_{xx}, \tag{A.2}$$

$$p_t + \gamma p v_x + v p_x = (\gamma - 1)(2\mu + \lambda) v_x^2 + \kappa (\gamma - 1) \mathrm{T}_{xx}. \tag{A.3}$$

We decompose each variable into its exact (known smooth and bounded) solution and a small smooth perturbation: $\rho = \rho_{\mathrm{ex}} + \rho'$, etc.

$$(\rho_{\mathrm{ex}} + \rho')_t + \big((\rho_{\mathrm{ex}} + \rho')(v_{\mathrm{ex}} + v')_x\big) = 0,$$

$$(\rho_{\mathrm{ex}})_t + \rho'_t + \big(\rho_{\mathrm{ex}} v_{\mathrm{ex}} + \rho_{\mathrm{ex}} v' + \rho' v_{\mathrm{ex}} + \rho' v'\big)_x = 0,$$

$$(\rho_{\mathrm{ex}})_t + \rho'_t + (\rho_{\mathrm{ex}} v_{\mathrm{ex}})_x + (\rho_{\mathrm{ex}})_x v' + \rho_{\mathrm{ex}} v'_x + \rho'_x v_{\mathrm{ex}} + \rho'(v_{\mathrm{ex}})_x + \rho'_x v' + \rho' v'_x = 0.$$

By definition $(\rho_{\mathrm{ex}})_t + (\rho_{\mathrm{ex}} v_{\mathrm{ex}})_x = 0$, and hence

$$\rho'_t + \underline{(\rho_{\mathrm{ex}})_x v'} + \rho_{\mathrm{ex}} v'_x + \rho'_x v_{\mathrm{ex}} + \underline{\rho'(v_{\mathrm{ex}})_x} + \rho'_x v' + \rho' v'_x = 0.$$

The underlined terms are zeroth-order derivatives of ρ' and v', and hence do not affect the well-posedness of the problem (see [9]), hence they are omitted. The linearisation is done by neglecting non-linear terms, i.e. $\rho'_x v' + \rho' v'_x$. The final result is

$$\rho'_t + \rho_{\mathrm{ex}} v'_x + v_{\mathrm{ex}} \rho'_x = 0.$$

For the velocity equation, we have

$$(v_{\text{ex}} + v')_t + (v_{\text{ex}} + v')(v_{\text{ex}} + v')_x + \frac{1}{\rho_{\text{ex}} + \rho'}(p_{\text{ex}} + p')_x = \frac{2\mu + \lambda}{\rho_{\text{ex}} + \rho'}(v_{\text{ex}} + v')_{xx},$$

$$(v_{\text{ex}})_t + v'_t + v_{\text{ex}}(v_{\text{ex}})_x + v_{\text{ex}}v'_x + v'(v_{\text{ex}})_x + v'v'_x + \frac{(p_{\text{ex}})_x}{\rho_{\text{ex}} + \rho'} + \frac{p'_x}{\rho_{\text{ex}} + \rho'} = (2\mu + \lambda)\left(\frac{(v_{\text{ex}})_{xx}}{\rho_{\text{ex}} + \rho'} + \frac{v'_{xx}}{\rho_{\text{ex}} + \rho'}\right).$$

Factorise $\frac{1}{\rho_{\text{ex}} + \rho'} = \frac{1}{\rho_{\text{ex}}}\frac{1}{1 + \frac{\rho'}{\rho_{\text{ex}}}}$, and Taylor expand the second factor; $\frac{1}{1 + \frac{\rho'}{\rho_{\text{ex}}}} = 1 - \frac{\rho'}{\rho_{\text{ex}}} + \mathcal{O}((\rho'/\rho_{\text{ex}})^2)$. Using that the exact solution satisfies Equation (A.2), we have

$$v'_t + v_{\text{ex}}v'_x + v'(v_{\text{ex}})_x + v'v'_x + (p_{\text{ex}})_x\left(-\frac{\rho'}{\rho_{\text{ex}}^2} + \mathcal{O}(\rho'/\rho_{\text{ex}}^2)\right) + p'_x\left(\frac{1}{\rho_{\text{ex}}} - \frac{\rho'}{\rho_{\text{ex}}^2} + \mathcal{O}(\rho'/\rho_{\text{ex}}^2)\right),$$

$$= (2\mu + \lambda)\left((v_{\text{ex}})_{xx}\left(-\frac{\rho'}{\rho_{\text{ex}}^2} + \mathcal{O}((\rho')^2/\rho_{\text{ex}}^3)\right) + v'_{xx}\left(\frac{1}{\rho_{\text{ex}}} - \frac{\rho'}{\rho_{\text{ex}}^2} + \mathcal{O}((\rho')^2/\rho_{\text{ex}}^3)\right)\right).$$

We neglect the non-linear terms and omit zeroth-order terms. This yields

$$v'_t + v_{\text{ex}}v'_x + \frac{p'_x}{\rho_{\text{ex}}} = \frac{2\mu + \lambda}{\rho_{\text{ex}}}v'_{xx}.$$

In the same way, the equation (A.3) becomes

$$(p_{\text{ex}} + p')_t + \gamma(p_{\text{ex}} + p')(v + v')_x + (v_{\text{ex}} + v')(p_{\text{ex}} + p')_x$$
$$= (\gamma - 1)(2\mu + \lambda)(v_{\text{ex}} + v')_x^2 + \kappa(\gamma - 1)(T_{\text{ex}} + T')_{xx},$$

that after expansion becomes,

$$(p_{\text{ex}})_t + p'_t + \gamma(p_{\text{ex}})(v_{\text{ex}})_x + \gamma(p_{\text{ex}})v'_x + \gamma p'(v_{\text{ex}})_x + \gamma p'v'_x + v_{\text{ex}}(p_{\text{ex}})_x + v_{\text{ex}}p'_x + v'(p_{\text{ex}})_x + v'p'_x,$$
$$= (\gamma - 1)(2\mu + \lambda)\left((v_{\text{ex}})_x^2 + 2(v_{\text{ex}})_x v'_x + v'^2_x\right) + \kappa(\gamma - 1)(T_{\text{ex}} + T)_{xx}.$$

Next, consider the linearisation of the temperature

$$\mathcal{R}((T_{\text{ex}})_{xx} + T'_{xx}) = \frac{(p_{\text{ex}})_{xx} + p'_{xx}}{\rho_{\text{ex}} + \rho'} - 2\frac{((p_{\text{ex}})_x + p'_x)((\rho_{\text{ex}})_x + \rho'_x)}{(\rho_{\text{ex}} + \rho')^2}$$
$$+ 2\frac{(p_{\text{ex}} + p')((\rho_{\text{ex}})_x + \rho'_x)^2}{(\rho_{\text{ex}} + \rho')^3} - \frac{(p_{\text{ex}} + p')((\rho_{\text{ex}})_{xx} + \rho'_{xx})}{(\rho_{\text{ex}} + \rho')^2},$$
$$= \frac{(p_{\text{ex}})_{xx} + p'_{xx}}{\rho_{\text{ex}} + \rho'} - 2\frac{(p_{\text{ex}})_x(\rho_{\text{ex}})_x + (p_{\text{ex}})_x\rho'_x + p'_x(\rho_{\text{ex}})_x + p'_x\rho'_x}{(\rho_{\text{ex}} + \rho')^2}$$
$$+ 2\frac{p_{\text{ex}}(\rho_{\text{ex}})_x^2 + 2p_{\text{ex}}(\rho_{\text{ex}})_x\rho'_x + p_{\text{ex}}\rho'^2_x + p'(\rho_{\text{ex}})_x^2 + 2p'(\rho_{\text{ex}})_x\rho'_x + p'\rho'^2_x}{(\rho_{\text{ex}} + \rho')^3}$$
$$- \frac{p_{\text{ex}}(\rho_{\text{ex}})_{xx} + p_{\text{ex}}\rho'_{xx} + p'(\rho_{\text{ex}})_{xx} + p'\rho'_{xx}}{(\rho_{\text{ex}} + \rho')^2}.$$

Taylor expanding yields

$$\mathcal{R}((T_{\text{ex}})_{xx} + T'_{xx})$$
$$= ((p_{\text{ex}})_{xx} + p'_{xx})\left(\frac{1}{\rho_{\text{ex}}} - \frac{\rho'}{\rho_{\text{ex}}^2} + \mathcal{O}((\rho')^2/\rho_{\text{ex}}^3)\right)$$
$$- 2\left((p_{\text{ex}})_x(\rho_{\text{ex}})_x + (p_{\text{ex}})_x\rho'_x + p'_x(\rho_{\text{ex}})_x + p'_x\rho'_x\right)\left(\frac{1}{\rho_{\text{ex}}^2} - \frac{\rho'}{\rho_{\text{ex}}^3} + \mathcal{O}((\rho')^2/\rho_{\text{ex}}^4)\right)$$
$$+ 2\left(p_{\text{ex}}(\rho_{\text{ex}})_x^2 + 2p_{\text{ex}}(\rho_{\text{ex}})_x\rho'_x + p_{\text{ex}}\rho'^2_x + p'(\rho_{\text{ex}})_x^2 + 2p'(\rho_{\text{ex}})_x\rho'_x + p'\rho'^2_x\right)\left(\frac{1}{\rho_{\text{ex}}^3} - \frac{\rho'}{\rho_{\text{ex}}^4} + \mathcal{O}((\rho')^2/\rho_{\text{ex}}^5)\right)$$
$$- \left(p_{\text{ex}}(\rho_{\text{ex}})_{xx} + p_{\text{ex}}\rho'_{xx} + p'(\rho_{\text{ex}})_{xx} + p'\rho'_{xx}\right)\left(\frac{1}{\rho_{\text{ex}}^2} - \frac{\rho'}{\rho_{\text{ex}}^3} + \mathcal{O}((\rho')^2/\rho_{\text{ex}}^4)\right).$$

The exact solution disappears and the quadratic terms are neglected in the linearisation procedure to obtain

$$\mathcal{R}\mathrm{T}'_{xx} = \frac{p'_{xx}}{\rho_{\mathrm{ex}}} - 2\frac{(p_{\mathrm{ex}})_x\rho'_x + p'_x(\rho_{\mathrm{ex}})_x}{\rho_{\mathrm{ex}}^2} + \frac{4p_{\mathrm{ex}}(\rho_{\mathrm{ex}})_x\rho'_x}{\rho_{\mathrm{ex}}^3} - \frac{p_{\mathrm{ex}}\rho'_{xx}}{\rho_{\mathrm{ex}}^2}.$$

Turning back to the pressure equation, and using that the exact solution satisfies (A.3), we end up with

$$p'_t + \gamma(p_{\mathrm{ex}})v'_x + \gamma p'(v_{\mathrm{ex}})_x + \gamma p'v'_x + v_{\mathrm{ex}}p'_x + v'(p_{\mathrm{ex}})_x + v'p'_x,$$
$$= (\gamma - 1)(2\mu + \lambda)\left(2(v_{\mathrm{ex}})_x v'_x + v'^2_x\right) + \kappa(\gamma - 1)\mathrm{T}'_{xx}.$$

Since non-principal parts of the viscous flux can be bounded by the principal part in the interior and do not affect the number of boundary conditions needed for linear well-posedness, we drop them together with all non-linear terms, and obtain

$$p'_t + \gamma p_{\mathrm{ex}}v'_x + v_{\mathrm{ex}}p'_x = \frac{\kappa}{\mathcal{R}}(\gamma - 1)\left(\frac{p'_{xx}}{\rho_{\mathrm{ex}}} - \frac{p}{\rho_{\mathrm{ex}}^2}\rho'_{xx}\right).$$

Next, we freeze the coefficients (the exact solutions), and denote them by the superscript star. We end up with the linearised system

$$\rho'_t + v^*\rho'_x + \rho^*v'_x = 0,$$
$$v'_t + v^*v'_x + \frac{1}{\rho^*}p'_x = \frac{2\mu+\lambda}{\rho^*}v'_{xx},$$
$$p'_t + \gamma p^*v'_x + v^*p'_x = -\frac{\gamma\mu p^*}{\mathrm{Pr}\rho^{*2}}\rho'_{xx} + \frac{\gamma\mu}{\mathrm{Pr}\rho}p'_{xx}.$$

(This is the starting point in [1].)

A.2. Linearised gas law

Recall that $p = \rho\mathcal{R}\mathrm{T}$. By the same procedure as above, we linearise this gas law as follows

$$p_{\mathrm{ex}} + p' = \mathcal{R}\left(\rho_{\mathrm{ex}} + \rho'\right)\left(\mathrm{T}_{\mathrm{ex}} + \mathrm{T}'\right) = \mathcal{R}\left(\rho_{\mathrm{ex}}\mathrm{T}_{\mathrm{ex}} + \rho_{\mathrm{ex}}\mathrm{T}' + \rho'\mathrm{T}_{\mathrm{ex}} + \rho'\mathrm{T}'\right).$$

Since $p_{\mathrm{ex}} = \mathcal{R}\rho_{\mathrm{ex}}\mathrm{T}_{\mathrm{ex}}$, by neglecting the non-linear term $\mathcal{R}\rho'\mathrm{T}'$, this reduces to

$$p' = \mathcal{R}\left(\rho_{\mathrm{ex}}\mathrm{T}' + \rho'\mathrm{T}_{\mathrm{ex}}\right).$$

Solving for T' and freezing the coefficients yields

$$\mathrm{T}' = \frac{1}{\mathcal{R}}\left(\frac{p'}{\rho^*} - \frac{p^*\rho'}{\rho^{*2}}\right).$$

Appendix B. Kronecker products

Let $\tilde{B}_N$ be the $(N+1) \times (N+1)$ matrix given by

$$\tilde{B}_N = \begin{pmatrix} 0 & -\frac{1}{2} & 0 & 0 & 0 & \dots & 0 \\ -\frac{1}{2} & 0 & 0 & 0 & 0 & \dots & 0 \\ 0 & 0 & 0 & 0 & 0 & \dots & 0 \\ \vdots & & & \ddots & & & \vdots \\ 0 & \dots & 0 & 0 & 0 & 0 & 0 \\ 0 & \dots & 0 & 0 & 0 & 0 & \frac{1}{2} \\ 0 & \dots & 0 & 0 & 0 & \frac{1}{2} & 0 \end{pmatrix},$$

and $\tilde{B}_M$ the $(M+1) \times (M+1)$ matrix with the same form as $\tilde{B}_N$. Furthermore, let $\tilde{H}_x = H_x\tilde{I}_N$, where $H_x = h_x \cdot \mathrm{diag}(1/2, 1, \dots, 1, 1/2)$ and $\tilde{I}_N$ is the $(N+1) \times (N+1)$ identity matrix, with the upper left and lower right element set to zero. $\tilde{H}_y$ is defined similarly (see Section 5.6).

Next, for a two-dimensional grid, the solution vectors are ordered as

$$\boldsymbol{u}^T = \left(\boldsymbol{u}^T_{i,1} \quad \boldsymbol{u}^T_{i,1} \quad \boldsymbol{u}^T_{i,2} \quad \dots \quad \boldsymbol{u}^T_{i,M}\right),$$

where $\boldsymbol{u}^T_{i,j} = \left(u_{0,j} \quad u_{1,j} \quad u_{2,j} \quad \dots \quad u_{N,j}\right)$. This more compact form of writing the vectors will be convenient below.

The Kronecker products, $\tilde{H}_y \otimes \tilde{B}_N$ and $\tilde{B}_M \otimes \tilde{H}_x$ written as matrices can be stated more compactly in the following way

$$
\tilde{H}_y \otimes \tilde{B}_N = h_y
\begin{pmatrix}
\mathbf{0} & \mathbf{0} & \mathbf{0} & \mathbf{0} & \dots & \mathbf{0} \\
\mathbf{0} & \begin{pmatrix} 0 & -\frac{1}{2} & \dots & 0 \\ -\frac{1}{2} & 0 & \dots & 0 \\ 0 & \dots & 0 & \frac{1}{2} \\ 0 & \dots & \frac{1}{2} & 0 \end{pmatrix} & \mathbf{0} & \mathbf{0} & \dots & \mathbf{0} \\
\mathbf{0} & \mathbf{0} & \begin{pmatrix} 0 & -\frac{1}{2} & \dots & 0 \\ -\frac{1}{2} & 0 & \dots & 0 \\ 0 & \dots & 0 & \frac{1}{2} \\ 0 & \dots & \frac{1}{2} & 0 \end{pmatrix} & \mathbf{0} & \dots & \mathbf{0} \\
\vdots & & & \ddots & & \vdots \\
\vdots & & & & \ddots & \vdots \\
\mathbf{0} & \dots & \mathbf{0} & \mathbf{0} & \mathbf{0} & \mathbf{0}
\end{pmatrix},
$$

$$
\tilde{B}_M \otimes \tilde{H}_x = h_x
\begin{pmatrix}
\mathbf{0} & -\frac{1}{2}\begin{pmatrix} 0 & 0 & 0 & \dots & 0 \\ 0 & 1 & 0 & \dots & 0 \\ & & \ddots & & \\ 0 & \dots & 0 & 1 & 0 \\ 0 & \dots & 0 & 0 & 0 \end{pmatrix} & \mathbf{0} & \mathbf{0} & \mathbf{0} & \dots & \mathbf{0} \\
-\frac{1}{2}\begin{pmatrix} 0 & 0 & 0 & \dots & 0 \\ 0 & 1 & 0 & \dots & 0 \\ & & \ddots & & \\ 0 & \dots & 0 & 1 & 0 \\ 0 & \dots & 0 & 0 & 0 \end{pmatrix} & \mathbf{0} & \mathbf{0} & \mathbf{0} & \mathbf{0} & \dots & \mathbf{0} \\
\mathbf{0} & \mathbf{0} & \mathbf{0} & \mathbf{0} & \mathbf{0} & \dots & \mathbf{0} \\
\vdots & & & \ddots & & & \vdots \\
\mathbf{0} & \dots & \mathbf{0} & \mathbf{0} & \mathbf{0} & \dots & \mathbf{0} \\
\mathbf{0} & \dots & \mathbf{0} & \mathbf{0} & \mathbf{0} & \frac{1}{2}\begin{pmatrix} 0 & 0 & 0 & \dots & 0 \\ 0 & 1 & 0 & \dots & 0 \\ & & \ddots & & \\ 0 & \dots & 0 & 1 & 0 \\ 0 & \dots & 0 & 0 & 0 \end{pmatrix} & \mathbf{0} \\
\mathbf{0} & \dots & \mathbf{0} & \mathbf{0} & \mathbf{0} & \frac{1}{2}\begin{pmatrix} 0 & 0 & 0 & \dots & 0 \\ 0 & 1 & 0 & \dots & 0 \\ & & \ddots & & \\ 0 & \dots & 0 & 1 & 0 \\ 0 & \dots & 0 & 0 & 0 \end{pmatrix} & \mathbf{0} & \mathbf{0}
\end{pmatrix},
$$

where the bold-face zero denotes a matrix of size $(N + 1) \times (N + 1)$ with all elements being zero.

Applying these products to a vector, $\boldsymbol{u}$, yields

$$(\tilde{H}_y \otimes \tilde{B}_N)\boldsymbol{u} = h_y \begin{pmatrix} \underline{\mathbf{0}} & \tilde{B}_N \boldsymbol{u}_{i,1} & \tilde{B}_N \boldsymbol{u}_{i,2} & \dots & \tilde{B}_N \boldsymbol{u}_{i,M-1} & \underline{\mathbf{0}} \end{pmatrix}^T, \tag{B.1}$$

$$(\tilde{B}_M \otimes \tilde{H}_x)\boldsymbol{u} = \begin{pmatrix} -\frac{1}{2}\tilde{H}_x \boldsymbol{u}_{i,1} & -\frac{1}{2}\tilde{H}_x \boldsymbol{u}_{i,0} & \underline{\mathbf{0}} & \dots & \underline{\mathbf{0}} & \frac{1}{2}\tilde{H}_x \boldsymbol{u}_{i,M} & \frac{1}{2}\tilde{H}_x \boldsymbol{u}_{i,M-1} \end{pmatrix}^T. \tag{B.2}$$

Note that in the above expressions, the underlined bold-face zeros denotes vectors of length $N + 1$ with all elements being zero.

References

[1] S. Abarbanel, D. Gottlieb, Optimal time splitting for two- and three-dimensional Navier-Stokes equations with mixed derivatives, J. Comput. Phys. 41 (1) (1981) 1–33, https://doi.org/10.1016/0021-9991(81)90077-2.

[2] M.H. Carpenter, D. Gottlieb, S. Abarbanel, Time-stable boundary conditions for finite-difference schemes solving hyperbolic systems: methodology and application to high-order compact schemes, J. Comput. Phys. 111 (1994) 220–236.

[3] J. Chan, Y. Lin, T. Warburton, Entropy stable modal discontinuous Galerkin schemes and wall boundary conditions for the compressible Navier-Stokes equations, J. Comput. Phys. 448 (2022), https://doi.org/10.1016/j.jcp.2021.110723.

[4] L. Dalcin, D. Rojas, S. Zampini, D.C.D.R. Fernández, M.H. Carpenter, M. Parsani, Conservative and entropy stable solid wall boundary conditions for the compressible Navier-Stokes equations: adiabatic wall and heat entropy transfer, J. Comput. Phys. 397 (2019) 108775, https://doi.org/10.1016/j.jcp.2019.06.051.

[5] D.C.D.R. Fernández, J.E. Hicken, D.W. Zingg, Review of summation-by-parts operators with simultaneous approximation terms for the numerical solution of partial differential equations, Comput. Fluids 95 (2014) 171–196, https://doi.org/10.1016/j.compfluid.2014.02.016.

[6] G.J. Gassner, M. Svärd, F.J. Hindenlang, Stability issues of entropy-stable and/or split form high-order schemes, J. Sci. Comput. 90 (79) (2022), https://doi.org/10.1007/s10915-021-01720-8.

[7] S. Gottlieb, On high order strong stability preserving Runge-Kutta and multi step time discretizations, J. Sci. Comput. 25 (1) (2005), https://doi.org/10.1007/s10915-004-4635-5.

[8] B. Gustafsson, High Order Difference Methods for Time Dependent PDE, Springer Series in Computational Mathematics, Springer-Verlag Berlin Heidelberg, ISBN 978-3-540-74993-6, 2008.

[9] B. Gustafsson, H.-O. Kreiss, J. Oliger, Time-Dependent Problems and Difference Methods, 2nd edition, Pure and Applied Mathematics, John Wiley & Sons, Inc., ISBN 978-0-470-90056-7, 2013.

[10] A. Harten, On the symmetric form of systems of conservation laws with entropy, J. Comput. Phys. 49 (1983) 151–164.

[11] T.J.R. Hughes, L. Franca, M. Mallet, A new finite element formulation for computational fluid dynamics: I. Symmetric forms of the compressible Euler and Navier-Stokes equations and the second law of thermodynamics, Comput. Methods Appl. Mech. Eng. 54 (1986) 223–234, https://doi.org/10.1016/0045-7825(86)90127-1.

[12] K.O. Friedrichs, P.D. Lax, System of conservation equations with a convex extension, Proc. Natl. Acad. Sci. USA 68 (8) (1971) 1686–1688.

[13] H.-O. Kreiss, J. Lorenz, Initial-Boundary Value Problems and the Navier-Stokes Equations, Academic Press, ISBN 0-89871-565-2, 1989.

[14] H.O. Kreiss, G. Scherer, Finite element and finite difference methods for hyperbolic partial differential equations, in: Mathematical Aspects of Finite Elements in Partial Differential Equations, 1974.

[15] H.O. Kreiss, L. Wu, On the stability definition of difference approximations for the initial boundary value problem, Appl. Numer. Math. 12 (1993) 213–227.

[16] K. Mattsson, J. Nordström, Summation by parts operators for finite difference approximations of second derivatives, J. Comput. Phys. 199 (2004) 503–540, https://doi.org/10.1016/j.jcp.2004.03.001.

[17] K. Mattsson, M. Svärd, J. Nordström, Stable and accurate artificial dissipation, J. Sci. Comput. 21 (1) (2004).

[18] K. Mattsson, F. Ham, G. Iaccarino, Stable and accurate wave-propagation in discontinuous media, J. Comput. Phys. 227 (2008) 8753–8767, https://doi.org/10.1016/j.jcp.2008.06.0.

[19] K. Mattsson, M. Svärd, M. Shoeybi, Stable and accurate schemes for the compressible Navier-Stokes equations, J. Comput. Phys. 227 (2008) 2293–2316, https://doi.org/10.1016/j.jcp.2007.10.018.

[20] S. Mishra, M. Svärd, On stability of numerical schemes via frozen coefficients and the magnetic induction equations, BIT Numer. Math. 50 (1) (2010) 85–108, https://doi.org/10.1007/s10543-010-0249-5.

[21] J. Nordström, K. Forsberg, C. Adamsson, P. Eliasson, Finite volume methods, unstructured meshes and strict stability for hyperbolic problems, Appl. Numer. Math. 45 (2003) 453–473.

[22] J. Nordström, S. Eriksson, P. Eliasson, Weak and strong wall boundary procedures and convergence to steady-state of the Navier-Stokes equations, J. Comput. Phys. 231 (2012) 4867–4884, https://doi.org/10.1016/j.jcp.2012.04.007.

[23] M. Parsani, M.H. Carpenter, E.J. Nielsen, Entropy stable wall boundary conditions for the three-dimensional compressible Navier-Stokes equations, J. Comput. Phys. 292 (2015) 88–113, https://doi.org/10.1016/j.jcp.2015.03.026.

[24] G. Strang, Accurate partial difference methods II. Non-linear problems, Numer. Math. 6 (1964) 37–46.

[25] M. Svärd, A convergent numerical scheme for the compressible Navier-Stokes equations, SIAM J. Numer. Anal. 54 (3) (2016) 1484–1506.

[26] M. Svärd, A new Eulerian model for viscous and heat conducting compressible flows, Physica A 506 (2018) 350–375, https://doi.org/10.1016/j.physa.2018.03.097.

[27] M. Svärd, Entropy stable boundary conditions for the Euler equations, J. Comput. Phys. (2020), https://doi.org/10.1016/j.jcp.2020.109947.

[28] M. Svärd, J. Nordström, A stable high-order finite difference scheme for the compressible Navier-Stokes equations, no-slip wall boundary conditions, J. Comput. Phys. 227 (2008) 4805–4824, https://doi.org/10.1016/j.jcp.2007.12.028.

[29] M. Svärd, J. Nordström, Review of summation-by-parts schemes for initial-boundary-value problems, J. Comput. Phys. 268 (2014) 17–38, https://doi.org/10.1016/j.jcp.2014.02.031.

[30] M. Svärd, M.H. Carpenter, J. Nordström, A stable high-order finite difference scheme for the compressible Navier-Stokes equations, far-field boundary conditions, J. Comput. Phys. 225 (2007) 1020–1038, https://doi.org/10.1016/j.jcp.2007.01.023.

[31] M. Svärd, M.H. Carpenter, M. Parsani, Entropy stability and the no-slip wall boundary condition, SIAM J. Numer. Anal. 56 (1) (2018) 256–273.

[32] E. Tadmor, Entropy stability theory for difference approximations of nonlinear conservation laws and related time-dependent problems, Acta Numer. (2003) 451–512, https://doi.org/10.1017/S0962492902000156.